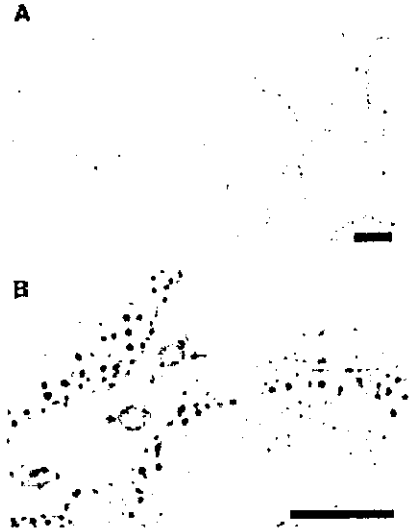

FIG. 2. Localization of CSE in the rat testis. (A) Low-power representative picture showing immunohistochemical analysis indicates the localization of CSE in the rat testis. (B) High-power representative picture showing the enzyme expression. Note the presence of CSE in Sertoli cells and immature germ cells standing close to the seminiferous tubules, whereas mature cells located in the central portion of the tubules exhibit little expression, if any. Note marked expression of CSE in vascular smooth muscle cells in the interstitial space (arrows in B). Bars = 100 μm.

suggest that both CBS and CSE did not alter greatly in response to the heavy metal stressor so far as judged from the protein expression.

Analyses of sulfur-containing amino acid metabolism and H_2S generation

Table 1 illustrates metabolomic profiles of alterations in contents of sulfur-containing amino acids and their derivatives in testes of $CdCl_2$-treated rats. Data were collected at 12 h after the administration of the reagent. As seen, administration of $CdCl_2$ induced a significant elevation of contents of methionine, SAH, serine, and cysteine. By contrast, contents of cystathionine and the oxidized form of glutathione (GSSG) were significantly decreased. On the other hand, terminal products of the transsulfuration pathway such as H_2S and taurine were unchanged in response to the exposure to $CdCl_2$. Homocysteine, a product standing at the intersection between remethylation and transsulfuration pathways, was undetectable in testicular samples so far as determined by the present analyses. The observation that testicular contents of cysteine were significantly elevated by the $CdCl_2$ exposure led us to examine if this event coincided with alterations in contents of sulfur-containing compounds in the plasma component. As seen in Table 2, the administration of $CdCl_2$ significantly decreased plasma contents of homocysteine and cysteine, while inducing no notable changes in glutathione. Interpretation of these events will be discussed later in the Discussion.

LS____
LE____
LL____

TABLE 1. ANALYSES OF SULFUR-CONTAINING AMINO ACID METABOLISM IN RAT TESTES TREATED WITH VEHICLE AND $CdCL_2$

Metabolites	*Vehicle*	*$CdCl_2$*
Remethylation metabolites		
Methionine	25.2 ± 2.8	114.6 ± 8.2*
S-Adenosylmethionine	24.1 ± 1.1	22.8 ± 2.3
S-Adenosylhomocysteine	1.6 ± 0.2	2.2 ± 0.1*
Homocysteine	ND	ND
Serine	427.4 ± 31.4	694.6 ± 63.7*
Transsulfuration metabolites		
Cystathionine	12.6 ± 0.7	9.4 ± 1.4*
Cysteine	29.5 ± 7.1	132.1 ± 16.5*
H_2S	19.6 ± 0.7	19.2 ± 1.8
GSH	2531 ± 89	2300 ± 79
GSSG	284 ± 14	128 ± 13*
Taurine	1,182 ± 140	1,021 ± 102

Data (in nmol/g of tissue) represent means ± SD of four to 13 separate experiments.
*$p < 0.05$ as compared with data collected from the vehicle-treated control rats.

As the contents of metabolites could be altered as a function of those of their upstream substrates, we analyzed the ratio values of the contents such as SAH/SAM and reduced glutathione (GSH)/GSSG to estimate alterations in methyl donation and redox regulation of glutathione, respectively. In addition, as H_2S is synthesized through the reactions of CBS and/or CSE, which consume cysteine as the common substrate, the ratio between H_2S and cysteine was calculated and compared between the control and cadmium-treated groups. As summarized in Fig. 3, total amounts of the substrates for the remethylation cycle in the cadmium-treated group became 2.5-fold greater than those of the control group. Under these circumstances, the SAH/SAM values were significantly elevated, suggesting acceleration of methyl donation in the cadmium-exposed testes. The cadmium exposure also turned out to elicit marked changes in the transsulfuration pathway. As indicated in a marked reduction of the H_2S/cysteine ratio, amounts of the gas generated in the tissue appeared to be far smaller than those expected from the elevation of cysteine contents. Another important change occurring at the transsul-

TABLE 2. ALTERATIONS IN PLASMA CONCENTRATIONS OF HOMOCYSTINE, CYSTEINE, AND GLUTATHIONE IN RAT TESTES TREATED WITH VEHICLE AND $CdCL_2$

Plasma concentrations	*Vehicle*	*$CdCl_2$*
Homocystine	9.8 ± 0.5	8.1 ± 0.5*
Cystine	178.8 ± 6.0	147.9 ± 4.0*
Glutathione	21.2 ± 0.9	19.6 ± 0.7

Data (in μmol/L) represent means ± SD of five or six separate experiments for each group.
*$p < 0.05$ as compared with data collected from the vehicle-treated control rats.

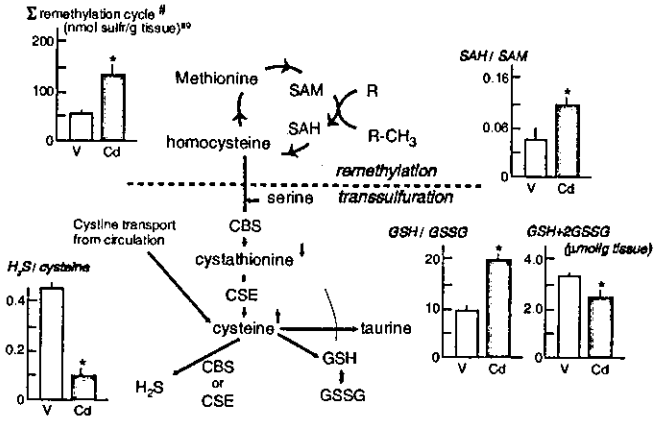

FIG. 3. Schematic diagram showing alterations in the remethylation and transsulfuration among rats treated with vehicle (V) and $CdCl_2$ (Cd). Σ remethylation*: the sum of the methionine, SAM, and SAH. Data indicate the means ± SD of separate experiments. $*p < 0.05$ as compared with data collected from control rats treated with vehicle.

furation processes is a modest decrease in total glutathione (GSH + 2GSSG), which coincided with a marked elevation of the GSH/GSSG ratio. Consequently, in the testes exposed to $CdCl_2$, H_2S generation is relatively down-regulated, whereas GSH appears to be well preserved. These results suggest that remodeling of sulfur-containing amino acids elicited by $CdCl_2$ involves preservation of the antioxidative capacity of glutathione.

DISCUSSION

This study first demonstrated distribution patterns of CSE and CBS in testes of rats. In this organ, these enzymes occurred in distinct topographic patterns. According to the classic concept for cysteine metabolism, CSE and CBS cooperatively execute biotransformation of sulfur-containing amino acids such as methionine into cysteine. In this context, Sertoli cells appear to play an important role in the amino acid metabolism, because both enzymes are colocalized with abundant expression. This fact is reasonable in that the cells are known to require ample amounts of glutathione to maintain their capacity to nurse germ cells for spermatogenesis (16, 18, 22). The anatomical distribution of these enzymes revealed in the current study led us to suggest putative pathways for methionine metabolism; because of its biochemical feature as an essential amino acid supplied through circulation from nutritional resources, methionine could access Sertoli cells directly or be captured primarily by Leydig cells to be converted to cystathionine and then secondarily transferred to Sertoli cells where both enzymes are colocalized.

Although such an intercellular pathway for amino acid transfer has not been investigated in the current study, the role of Leydig cells as a putative gateway to facilitate methionine metabolism is likely to be of great physiologic relevance. Previous studies revealed that testicular germ cells abundantly express antioxidative enzymes such as glutathione peroxidase and thioredoxin reductase (16, 23, 26). Considering that nutritional support via the bloodstream in the interstitial space plays a crucial role in maintenance of spermatogenesis, it is not unreasonable to speculate that both Leydig cells and Sertoli cells cooperatively execute the delivery of cysteine and H_2S as reductants to strengthen antioxidative capacity of the germ cells for a quality control of spermatogenesis.

To further clarify mechanisms for metabolic remodeling of sulfur-containing amino acid derivatives, we quantitatively determined the metabolites using metabolomic approaches. Metabolomic information that covers the whole products of remethylation and transsulfuration pathways led us to speculate the role of CBS as a critical enzymatic step causing the cadmium-induced changes in the metabolites; first, the exposure to $CdCl_2$ significantly expanded amounts of substrates for the remethylation cycle (Σ remethylation cycle) and appeared to facilitate methyl donation, as judged from the SAH/SAM ratio. Of importance is a reduction of the tissue cystathionine contents, suggesting the inhibition of the CBS activity. Despite such a decrease in the substrate for CSE, the cysteine contents were significantly elevated. Considering that cystine could access the intracellular space through the cystine transporter (11), the results suggest that the cadmium exposure could increase the testicular contents of cysteine through active uptake of the substrates from the circulation rather than through up-regulation of intratesticular delivery of the upstream substrate from the remethylation pathway. During these processes, maintenance of testicular H_2S concentration could help the entry of cysteine through the transporter (13).

As down-regulation of the enzyme *per se* secondarily greatly alters the expression of diverse genes (24), it is difficult to understand entire mechanisms for alterations in metabolites in the current experimental model (24). However, so far as judged from the aforementioned results, metabolome analyses given by the current study led us to hypothesize that CBS could serve as a putative target for the $CdCl_2$-induced remodeling of the methionine metabolism in the testes. Such a hypothesis is in good agreement with another observation that the ratio of H_2S/cysteine was significantly reduced upon the exposure. Recent studies suggest multiple mechanisms by which CBS alters its catalytic activities: such mechanisms involve proteolytic cleavage of the enzyme by cytokines (33) or modulation of the activity by binding of adenosine ligands to its CBS domain, suggesting the enzyme senses cellular energetics (25).

Another possible effector of the CBS activity is carbon monoxide (CO) derived from heme oxygenase, the gaseous monoxide that regulates neurovascular function (17, 19, 28). We have recently revealed that Leydig cells serve as a sensor for detecting exposure to heavy metal stressors such as cadmium and mediate down-regulation of spermatogenesis under stress conditions (22). To sense the stressors, the cells induce heme oxygenase-1 and increase CO as an alert signal for triggering germ cell apoptosis (22). Although molecular mechanisms by which CO tranduces signals involve soluble guanylate cyclase or mitogen-activated protein kinase, we recently collected evidence for the ability of the gas to inhibit the activity of CBS (Hoshikawa *et al.*, unpublished observations), in agreement with previous experiments using the purified CBS enzyme *in vitro* (31). If CO derived from Leydig cells could inhibit CBS in the same cells, biotransformation of methionine into cysteine and/or glutathione could largely be compromised to trigger germ cell apoptosis. Although further investigation is obviously necessary to specify which mechanisms could actually contribute to metabolic remodeling of the cadmium-exposed testes, the current results showed the potential usefulness of metabolomic approaches to pinpoint putative molecular candidates that play a critical role in metabolic regulation *in vivo*.

ACKNOWLEDGMENTS

AU: OK to add?

This study was supported by 21st Century Center-of-Excellence Program for Systems Biology and by Leading Project for Biosimulation from the Ministry of Education, Sciences and Technology of Japan.

ABBREVIATIONS

Ad4BP, adrenal 4 binding protein; CBS, cystathionine β-synthase; CO, carbon monoxide; CSE, cystathionine γ-lyase; GSH, reduced form of glutathione; GSSG, oxidized form of glutathione; H_2S, hydrogen sulfide; PBS, phosphate-buffered saline; SAH, *S*-adenosylhomocysteine; SAM, *S*-adenosylmethionine; TCA, trichloroacetic acid.

REFERENCES

1. Awata S, Nakayama K, Sato A, Kawamura M, Suzuki O, and Kodama H. Changes in cystathionine gamma lyase levels in rat liver during lactation. *Biochem Mol Biol Int* 31: 185–191, 1993.
2. Awata S, Nakayama K, Sato A, Kawamura M, Suzuki O, Sugahara H, and Kodama K. Degradation of cystathionine gamma-lyase in rat liver lysosomes: effect of leupetin treatment. *Biochem Mol Biol Int* 35: 1183–1187, 1995.
3. Bauche F, Fouchard MH, and Jegou B. Antioxidant system in rat testicular cells. *FEBS Lett* 349: 392–396, 1994.
4. de Oliveira AM, Pereira NR, Marsaioli A Jr, and Augusto F. Studies on the aroma of cupuassu liquor by headspace solid-phase microextraction and gas chromatography. *J Chromatogr A* 1025: 115–124, 2004.
5. Fujii K, Sakuragawa T, Kashiba M, Sugiura Y, Kondo M, Maruyama K, Goda N, Nimura Y, and Suematsu M. Hydrogen sulfide as an endogenous modulator of biliary bicarbonate excretion in the rat liver. *Antioxid Redox Signal* 7: xxx–xxx, 2005.
6. Goda N, Suzuki K, Naito M, Tsuchida E, Ishimura Y, Tamatani T, and Suematsu M. Distribution of heme oxygenase isoforms in rat liver: topographic basis for carbon monoxide-mediated microvascular relaxation. *J Clin Invest* 101: 604–610, 1998.
7. Hosoki R, Matsuki N, and Kimura H. The possible role of hydrogen sulfide as an endogenous smooth muscle relaxant in synergy with nitric oxide. *Biochem Biophys Res Commun* 237: 527–531, 1997.
8. Jones DP, Go YM, Anderson CL, Ziegler TR, Kinkade JM Jr, and Kirlin WG. Cysteine/cysteine couple is a newly recognized node in the circuitry for biologic redox signaling and control. *FASEB J* 18: 1246–1248, 2004.
9. Kang SW, Kang H, Park IS, Choi SH, Chun YS, Chun BG, and Min BH. Cytoprotective effect of arginine deiminase on taxol-induced apoptosis in DU145 human prostate cancer cells. *Mol Cells* 10: 331–337, 2000.
10. Kashiba M, Kajimura M, Goda N, and Suematsu M. From O_2 to H_2S: a landscape view of gas biology. *Kelo J Med* 51: 1–10, 2001.
11. Kim JY, Kanai Y, Chairoungdua A, Cha SH, Matsuo H, Kim DK, Inatomi J, Sawa H, Ida Y, and Endou H. Human cysteine/glutamate transporter: cDNA cloning and upregulation by oxidative stress in glioma cells. *Trends Pharmacol Sci* 23: 299–302, 2002.
12. Kimura H. Hydrogen sulfide induces cyclic AMP and modulates the NMDA receptor. *Biochem Biophys Res Commun* 267: 129–133, 2000.
13. Kimura Y and Kimura H. Hydrogen sulfide protects neurons from oxidative stress. *FASEB J* 18: 1165–1167, 2004
14. Kochakian CD. Free amino acids of sex organs of the mouse: regulation by androgen. *Am J Physiol* 228: 1231–1235, 1975.
15. Kraus J, Le K, Swaroop M, Ohura T, Tahara T, Rosenberg L, Roper M, and Kozich S. Human cystathionine beta synthase cDNA: sequence, alternative splicing and expression in cultured cells. *Hum Mol Genet* 2: 1633–1638, 1993.
16. Kumar TR, Wiseman AL, Kala G, Kala SV, Matzuk MM, and Lieberman NW. Reproductive defects in gamma-glutamyl transpeptidase-deficient mice. *Endocrinology* 141: 4270–4277, 2000.
17. Kyokane T, Norimizu S, Taniai H, Yamaguchi T, Takeoka S, Tsuchida E, Naito M, Nimura Y, Ishimura Y, and Suematsu M. Carbon monoxide from heme catabolism protects against hepatobiliary dysfunction in endotoxin-treated rat liver. *Gastroenterology* 120: 1227–1240, 2001.
18. Laskey JW and Phelps PV. Effect of cadmium and other metal cations on in vitro Leydig cell testosterone production. *Toxicol Appl Pharmacol* 108: 296–306, 1991.
19. Maines MD, Chung AS, and Kutty RK. The inhibition of testicular heme oxygenase activity by cadmium. A novel cellular response. *J Biol Chem* 257: 14116–14121, 1982.
20. Minniti G, Piana A, Armani U, and Cerone R. Determination of plasma and serum homocysteine by high-performance liquid chromatography with fluorescence detection. *J Chromatogr A* 828: 401–405, 1998.

LS____
LE____
LL____

21. Mukherjee SB, Aravinda S, Gopalakrishnan B, Nagpal S, Salunke DM, and Shaha C. Secretion of glutathione *S*-transferase isoforms in the seminiferous tubular fluid, tissue distribution and sex steroid binding by rat GSTM1. *Biochem J* 340: 309–320, 1999.
22. Ozawa N, Goda N, Makino N, Yamaguchi T, Yoshimura Y, and Suematsu M. Leydig cell-derived heme oxygenase-1 regulates apoptosis of premeiotic germ cells in response to stress. *J Clin Invest* 109: 457–467, 2002.
23. Ren XY, Zhou Y, Zhang JP, Feng WH, and Jiao BH. Expression of metallothionein gene at different time in testicular interstitial cells and liver of rats treated with cadmium. *World J Gastroenterol* 9: 1554–1558, 2003.
24. Robert K, Chasse JF, Santiard-Baron D, Vayssettes C, Chabli A, Aupetit J, Maeda N, Kamoun P, London J, and Janel N. Altered gene expression in liver from a murine model of hyperhomocysteinemia. *J Biol Chem* 278: 31504–31511, 2003.
25. Scott JW, Hawley SA, Green KA, Anis M, Stewart G, Scullion GA, Norman DG, and Hardie DG. CBS domains form energy-sensing modules whose binding of adenosine ligands is disrupted by disease mutations. *J Clin Invest* 113: 274–284, 2004.
26. Shubhada S, Daver R, and Tsai YH. The changing profiles of L-ornithine decarboxylase and *S*-adenosyl-L-methionine decarboxylase activities in testicular cell types during sexual maturation of male rats. *J Androl* 10: 152–158, 1989.
27. Suematsu M, Kashiwagi S, Sano T, Goda N, Shinoda Y, and Ishimura Y. Carbon monoxide as an endogenous modulator of hepatic vascular perfusion. *Biochem Biophys Res Commun* 205: 1333–1337, 1994.
28. Suematsu M, Goda N, Sano T, Kashiwagi S, Shinoda Y, and Ishimura Y. Carbon monoxide: an endogenous modulator of sinusoidal tone in the perfused rat liver. *J Clin Invest* 96: 2431–2437, 1995.
29. Suematsu M, Suganuma K, and Kashiwagi S. Mechanistic probing of gaseous signal transduction in microcirculation. *Antioxid Redox Signal* 5: 485–492, 2003.
30. Swaroop M, Bradley K, Ohura T, Tahara T, Roper MD, Rosenberg LE, and Kraus JP. Rat cystathionine beta synthase. Gene organization and alternative splicing. *J Biol Chem* 267: 11455–11461, 1992.
31. Taoka S and Banerjee R. Characterization of NO binding to human cystathionine beta-synthase. *J Inorg Biochem* 87: 245–251, 2001.
32. Zhao W, Ahang J, Lu Y, and Wang R. The vasorelaxant effect of H_2S as a novel endogenous gaseous K_{ATP} channel opener. *EMBO J* 20: 6008–6016, 2001.
33. Zou CG and Banerjee R. Tumor necrosis factor-alpha-induced targeted proteolysis of cystathionine beta synthase modulates redox homeostasis. *J Biol Chem* 278: 16802–16808, 2003.

Address reprint requests to:
Makoto Suematsu, M.D., Ph.D.
Professor and Chair
Department of Biochemistry and Integrative Medical Biology
School of Medicine, Keio University
35 Shinanomachi, Shinjuku-ku
Tokyo 160-8582, Japan

E-mail: msuem@sc.itc.keio.ac.jp

Received for publication December 3, 2004; accepted December 10, 2004.

___LS
___LE
___LL

Role of Thromboxane Derived From COX-1 and -2 in Hepatic Microcirculatory Dysfunction During Endotoxemia in Mice

Hiroyuki Katagiri,[1] Yoshiya Ito,[1] Ken-ichiro Ishii,[1] Izumi Hayashi,[2] Makoto Suematsu,[4] Shohei Yamashina,[3] Takahiko Murata,[5] Shuh Narumiya,[5] Akira Kakita,[1] and Masataka Majima[2]

Although thromboxanes (TXs), whose synthesis is regulated by cyclooxygenase (COX), have been suggested to promote inflammation in the liver, little is known about the role of TXA_2 in leukocyte endothelial interaction during endotoxemia. The present study was conducted to investigate the role of TXA_2 as well as that of COX in lipopolysaccharide (LPS)-induced hepatic microcirculatory dysfunction in male C57Bl/6 mice. We observed during *in vivo* fluorescence microscopic study that LPS caused significant accumulation of leukocytes adhering to the hepatic microvessels and non-perfused sinusoids. Levels of serum alanine transaminase (ALT) and tumor necrosis factor alpha (TNFα) also increased. LPS raised the TXB_2 level in the perfusate from isolated perfused liver. A TXA_2 synthase inhibitor, OKY-046, and a TXA_2 receptor antagonist, S-1452, reduced LPS-induced hepatic microcirculatory dysfunction by inhibiting TNFα production. OKY-046 suppressed the expression of an intercellular adhesion molecule (ICAM)-1 in an LPS-treated liver. In thromboxane prostanoid receptor-knockout mice, hepatic responses to LPS were minimized in comparison with those in their wild-type counterparts. In addition, a selective COX-1 inhibitor, SC-560, a selective COX-2 inhibitor, NS-398, and indomethacin significantly attenuated hepatic responses to LPS including microcirculatory dysfunction and release of ALT and TNFα. The effects of the COX inhibitors on hepatic responses to LPS exhibited results similar to those obtained with TXA_2 synthase inhibitor, and TXA_2 receptor antagonist. In conclusion, these results suggest that TXA_2 is involved in LPS-induced hepatic microcirculatory dysfunction partly through the release of TNFα, and that TXA_2 derived from COX-1 and COX-2 could be responsible for the microcirculatory dysfunction during endotoxemia. (HEPATOLOGY 2004;39:139–150.)

The initial hepatic responses to lipopolysaccharide (LPS) include the activation of the nonparenchymal cells that constitute the hepatic microvascular system. The early events occurring in the hepatic microvasculature, including increases in leukocyte adhesion, reduction of sinusoidal perfusion, and activated Kupffer cells contribute to alterations in liver function caused by endotoxin.[1,2] However, the mechanisms by which LPS induces hepatic microcirculatory dysfunction are not fully understood.

Proinflammatory cytokines released from activated Kupffer cells including tumor necrosis factor alpha (TNFα)[3,4] are involved in the hepatic microvascular inflammatory response to LPS. Inactivation of Kupffer cells with gadolinium chloride ameliorates LPS-induced hepatic microcirculatory dysfunction, and this process was accompanied by a decrease in the plasma TNFα level.[2] The administration of TNFα causes a hepatic microcirculatory derangement similar to that produced by endotoxin.[5] In addition to cytokines, metabolites of arachidonic acid including prostaglandins (PGs) and thromboxanes (TXs) have been suggested to participate in liver injury during endotoxemia.[6] For example, a significant increase in the plasma level of TXB_2 (a stable metabolite of TXA_2) is shown after LPS administration.[7] The TXA_2 receptor antagonist exerts a protective effect on

Abbreviations: LPS, lipopolysaccharide; TNF, tumor necrosis factor; PG, prostaglandin; TX, thromboxane; COX, cyclooxygenase; TP, thromboxane-prostanoid; ALT, alanine aminotransferase; RT-PCR, reverse-transcription polymerase chain reaction; ICAM-1, intercellular adhesion molecule-1; PECAM-1, platelet-endothelial cell adhesion molecule-1; mRNA, messenger RNA.

From the Departments of [1]Surgery, [2]Pharmacology, and [3]Anatomy, Kitasato University School of Medicine, Kanagawa, Japan; the [4]Department of Biochemistry and Integrative Medical Biology, Keio University, Tokyo, Japan; and the [5]Department of Pharmacology, Kyoto University, Kyoto, Japan.

Received January 17, 2003; accepted October 22, 2003.

Supported by grants from an Integrative Research Program of the Graduate School of Medical Science, Kitasato University, and from Parents' Association Grant of Kitasato University School of Medicine. This work was also supported by a research grant (#15390084), by a "High-tech Research Center" grant, and by a grant from The 21st Century COE Program, from Ministry of Education, Culture, Sports, Science and Technology (MEXT).

Address reprint requests to: Masataka Majima, Kitasato University School of Medicine, 1-15-1 Kitasato, Sagamihara, Kanagawa 228-8555, Japan. E-mail: en3m-mjm@asahi-net.or.jp; fax: +81-42-778-9556.

Published online in Wiley InterScience (www.interscience.wiley.com).

DOI 10.1002/hep.20000

liver injury caused by endotoxin.[8] Furthermore, PGs and TXs modulate TNFα synthesis. PGE_2 suppresses TNFα production from Kupffer cells stimulated with endotoxin,[9] while TXA_2 synthase inhibitor suppresses TNFα release from peritoneal macrophages.[7] These results suggest that TXA_2 could augment leukocyte-endothelial interaction during endotoxemia by affecting the production of TNFα.

The synthesis of TXA_2 is regulated by cyclooxygenase (COX), which catalyzes the conversion of arachidonic acid to PGs and TXs. Two isoforms of the enzyme have been identified. The isoform designated COX-1 is constitutively expressed in most tissues, while the isoform designated COX-2 is inducible by a variety of factors, such as cytokines and endotoxin.[10] Indeed, the expression of COX-2 protein was induced in LPS-treated liver from rats.[11] The liver injury caused by LPS sensitized with galactosamine was minimized in COX-2 deficient mice.[12] Inhibition of COX-2 protects the liver[13] against injury from ischemia/reperfusion. These results indicate that COX-2 contributes to liver injury. However, much remains unknown about the involvement of 2 isoforms of COX (COX-1 and COX-2) in hepatic microcirculatory dysfunction during endotoxemia.

The present study was thus conducted to examine the effects of the inhibition of TXA_2 synthase and of the blockade of TXA_2 receptor on the hepatic microvascular response to LPS in mice using *in vivo* microscopic methods. Some of the experiments were performed with thromboxane prostanoid (TP)-receptor knockout mice to elucidate the role of endogenously produced TXA_2 in this response. We also investigated the effects of selective inhibition of COX-1 and COX-2 on LPS-induced hepatic microcirculatory dysfunction.

Materials and Methods

Drugs. Endotoxin (LPS from *Escherichia coli*, serotype 055:B5) was purchased from List Biological Laboratories (Campbell, CA). The selective TXA_2 synthase inhibitor OKY-046 ((E)-3-[p-(1H-imidazolmethyl)-phenyl]-2-propenoic acid) was supplied from Kissei Pharmaceutical (Osaka, Japan). The TXA_2 receptor antagonist S-1452 (14) (calcium (1R, 2S, 3S, 4S)-(5Z)-7(((phenylsulphonyl)-amino)-bicyclo-(2.2.1)-hept-2-yl) hept-5-heptenoate dihydrate) was supplied by Shionogi Pharmaceutical (Osaka, Japan). The selective COX-1 inhibitor SC-560 (15) (5-(4-chlorophenyl)-1-(4-methoxyphenyl)-3-trifluoromethyl-pyrazole) was obtained from Searle (St. Louis, MO). The selective COX-2 inhibitor NS-398 (16) (N-[2-(cyclohexyloxy)-4-nitrophenyl]-methanesulfonamide) was obtained from Cayman Chemical (Ann Arbor, MI). The nonselective COX inhibitor indomethacin was purchased from Merck (Rahway, NJ). The NS-398, SC-560, indomethacin, and S-1452 were suspended in 5% gum arabic, while the OKY-046 was dissolved in physiological saline. Anti-mouse lymphocyte function associated antigen (LFA)-1 monoclonal antibody was purchased from Endogen (Woburn, MA).

Animals. Male C57BL/6 mice (6–8 weeks of age), weighing 20–25g, were obtained from Shizuoka Laboratory Animal Center (Hamamatsu, Japan). TP receptor-knockout mice ($TP^{-/-}$, male, 8 weeks of age) were developed by us.[17] A genetic background of TP-receptor knockout mice is similar to that of C57BL/6 mice. They were maintained at a constant humidity (60 ± 5%) and temperature (25 ± 1 °C) and were kept continuously on a 12-hour light/dark cycle. All animals were provided food and water *ad libitum*. All procedures on animals were performed in accordance with the guidelines for animal experiments of Kitasato University School of Medicine.

Experimental Protocols for* In Vivo *Microscopic Study. LPS was injected intravenously (0.3 mg/kg in 0.1 ml of physiological saline) into mice through the tail vein. OKY-046 (50 mg/kg in 0.1 ml saline, intravenously), S-1452 (10 mg/kg, per os), SC-560 (10 mg/kg, per os), NS-398 (10 mg/kg, subcutaneous injection), indomethacin (10 mg/kg, per os), and vehicle (10 mg/kg, per os) were administered 30 min before LPS injection. Some animals were treated with 2 mg/kg (intravenously) of the LFA-1 monoclonal antibody simultaneously with LPS injection. The dose regimens of the specific inhibitors, including NS-398 and SC-560, used in the present study were based on their inhibitory effects on activity against COX-1 or COX-2.[15,16]

Preparation for* In Vivo *Microscopy. Four hours after LPS injection, animals anesthetized with pentobarbital sodium (50 mg/kg, intraperitoneally) were prepared for *in vivo* fluorescence microscopy according to modifications of methods previously described.[5] After transverse laparotomy, the animals were positioned on their left side and placed on a stage. The left lobe of the liver was pulled gently and covered with a thin cover glass to stabilize its position and limit movement induced by respiration. The hepatic microcirculation was observed at the surface of the liver using a fluorescence microscope (X2-UD, upright type; Nikon, Tokyo) with a 100-W mercury lamp for epi-illumination. The microscopic images were obtained with a long working distance objective lens (M plan 20/0.20 SLWD; Nikon, Tokyo) and a ×5 eyepiece lens. Images of the hepatic microcirculation were transmitted through a silicon-intensified target camera (C2400-08; Hamamatsu Photonics; Hamamatsu) to a TV monitor screen (PVM-1444Q; Sony, Tokyo) and

were recorded on videotape with an S-VHS recorder (BR-S600; Victor, Tokyo).

For contrast enhancement of the plasma, FITC-labeled dextran (Sigma, St. Louis, MO) was intravenously administered (4 mg/kg) just before the start of the observation. Leukocytes were labeled with 0.3 μmol/kg of rhodamine-6G (Sigma) at the same time.[18] FITC-dextran and rhodamine-6G were visualized by epi-illumination with filter combination of 420 to 490 nm/ > 520 nm (excitation/emission) and 510 to 560 nm/ > 590 nm, respectively.

Analysis of* In Vivo *Microscopy. To examine the interaction of leukocytes with endothelium, the number of leukocytes adhering was determined off-line during video playback analysis. A leukocyte was defined as adhering to the venular and sinusoidal walls if it remained stationary for more than 20 seconds. With respect to the leukocytes adhering to the venules, 5 to 8 portal or central venules per animal were observed and assessed. The endothelial surface area of each venule was measured from video recordings using an adjustable electric microscaler (Argus-10; Hamamatsu Photonics; Hamamatsu). We determined the adherence of leukocytes in terms of 1) numbers of adhering leukocytes in the sinusoids per microscopic field (X100), and 2) numbers of adhering leukocytes in the portal and central venules per 1000 μm^2 of endothelial surface.

The sinusoidal perfusion deficits were evaluated by counting the number of non-perfused sinusoids in the same microscopic field as that in which the number of adhering leukocytes was determined. The percentage of non-perfused sinusoids was calculated as the ratio of the number of non-perfused sinusoids to the total number of all visible sinusoids. The results were expressed as the percentage of non-perfused sinusoids.

Sampling and Assays. In a separate set of experimental animals, blood was collected from the heart. The serum activity of alanine aminotransferase (ALT) was measured by an automated procedure with an analyzer. The plasma concentration of TNFα was measured with an enzyme-linked immunoabsorbent assay kit (Biosource International Inc, Camarillo, CA).

Experimental Procedure for Perfusion of the Isolated Liver. The isolated non-recirculating perfused liver system was prepared according to the method of Suematsu et al.[19] with some minor modification. In brief, mice were anesthetized with pentobarbital sodium (50 mg/kg, intraperitoneally) and were heparinized (100 units/mouse) to avoid blood coagulation in the liver. After transverse laparotomy, the portal vein was cannulated with a 24-gauge catheter. Immediately after the cannulation, the liver was initially perfused with a sterile, hemoglobin- and albumin-free Krebs-Henseleit bicarbonate buffered solution (pH 7.4, 37 °C) gassed with carbogen (95% O_2, 5% CO_2). After the start of perfusion of the liver, the inferior vena cava was cut, and the liver was removed. The perfusate was pumped through the isolated liver at a constant flow rate (4.0 ml/min) while the portal perfusion pressure was monitored and maintained at a level of 2 to 4 cmH_2O. Before collection of the first sample, the isolated liver was perfused for 20 min to eliminate blood elements and to stabilize it. Samples of the hepatic effluent emerging from the inferior vena cava were collected every 5 min to determine the amount of TXB_2. The levels of TXB_2 were measured with separate enzyme-linked immunoabsorbent assays (Cayman Chemical) as described previously.[20,21]

Experimental Protocols for Perfusion Experiment. Four experimental groups of animal livers were set up to investigate whether the liver is a site of TXA_2 production. In the 1st group, the livers of wild-type mice perfused with buffer solution throughout the experiment served as controls. In the 2nd and 3rd groups, 30 min after the start of perfusion, the administration of LPS (1.25 μg/min for 20 min) was initiated to TP-receptor knockout mice and to their wild-type counterparts and was continued throughout the experimental period. In the 4th group, 30 min before the start of preparation for the perfusion experiment, wild-type mice were treated with OKY-046 (50 mg/kg, intravenously), and OKY-046 (0.05 μg/min for 50 min) was administered simultaneously with the start of the perfusion with buffer. At 30 min after the start of perfusion, LPS (1.25 μg/min for 20 min) was continuously infused until the end of the experimental period.

Reverse-Transcription Polymerase Chain Reaction Analysis. Four hours after LPS injection, approximately 100 mg of the liver tissue was excised and was homogenized in 1 ml of Trizol Reagent (GIBCO BRL, Rockville, MD) with Polytrone (Kinematica GmbH, Luzern, Switzerland). A sample of RNA was extracted from the tissue in accordance with the manufacturer's instructions. Single-stranded complementary DNA was synthesized from 250 ng of total RNA using 0.4 μg of oligo-p(dT)15 primer and 4 units of AMV reverse transcriptase (Roche Diagnostics, Basel, Switzerland). PCR was performed in 10 μl of 20 mM Tris-HCl (pH 8.7) and 0.5 unit of Taq DNA polymerase (Qiagen GmbH, Germany). The oligonucleotide primers used were for reverse-transcription polymerase chain reaction (RT-PCR) analysis as follows: for mouse COX-1, 5′-TTGCACAACACTTCACCCACCAG–3′ (sense), 5′-AAACACCTCCTGGCCCACAGCCAT–3′ (antisense) (276 bp); mouse COX-2, 5′-GGAGAGAAGGAAATGGCTGCA–3′ (sense), 5′-ATCTAGTCTGGAGTGGGAGG–3′ (antisense) (363

bp); intercellular adhesion molecule (ICAM)-1, 5′-CGGGATCCAGGAAAGCCAAGGCCAAA-3′ (sense) and5′-CGGAATTCTTGACTGTCTTAA-GTTCC-3′ (antisense) (326 bp); platelet-endothelial cell adhesion molecule (PECAM)-1, 5′-CGGGATCCAG-GAAAGCCAAGGCCAAA-3′ (sense) and 5′-CG-GAATTCTTGACTGTCTTAAGTTCC-3′ (antisense) (348 bp); glyceraldehyde-3-phosphate dehydrogenase (GAPDH), 5′-CCCTTATTGACCTCAACTACAT-GGT-3′ (sense) and 5′-GAGGGGCCATCCACA-GTCTTCTG-3′ (antisense) (470 bp). These PCRs were run for 40 cycles. Cycling conditions were: 94 °C, 30 sec; 54 °C, 45 sec; and 72 °C, 45 sec for COX-1, ICAM-1, PECAM-1 and GAPDH, followed by a final extension for 10 min at 72 °C. For the amplification of COX-2, annealing was performed at 50 °C for 45 sec. Products of PCR were analyzed using 1.8% agarose gel electrophoresis, and the size of products was predicted from the sequences.

Immunohistochemical Studies. Immunohistochemical studies were performed as described elsewhere[22]. The sections from the paraffin-embedded tissues were incubated with rabbit anti-murine COX-1 or COX-2 antiserum (1:200 dilution, Cayman), or with rat anti-murine ICAM-1 antibody (1:100 dilution, 1A29, Biotechnology, Oxford) or rat anti-murine PECAM-1 antibody (1:100 dilution, MEC 13.3, PharMingen) at 4 °C overnight. These immunoreactivities were visualized using avidin-biotin-peroxydase complex (Vectastain ABC Kit, Vector Lab., Burlingame, CA).

Statistical Analysis. All data were expressed as means ± SEM. Multiple comparisons were carried out using 1-way ANOVA followed by Fisher's test. Differences were considered to be significant for P values less than .05.

Results

Figure 1 shows the *in vivo* fluorescence micrographs of hepatic microvasculature 4 hours after LPS injection. Leukocytes were seen adhering to the sinusoids as well as to the central venules (Fig. 1A). The sinusoidal perfusion deficits were also observed (Fig. 1B). In an additional group of experiments, we observed that the mean systemic arterial blood pressure 4 hours after LPS injection (109.3 ± 5.4 mmHg) did not change significantly when compared with that before LPS treatment (107.5 ± 5.6 mmHg) (n = 4).

The administration of LPS caused significant increases in the numbers of leukocytes adhering to the portal venules (8.5-fold) (Fig. 2A), sinusoids (50.2-fold) (Fig. 2B), and central venules (51.0-fold) (Fig. 2C) in comparison with those in saline-treated mice. Pre-treatment with OKY-046 lowered those by 61%, 46%, and 45.0%, respectively. Pre-treatment with S-1452 also suppressed those by 69%, 48%, and 39.0%, respectively. Concomitantly, the percentage of non-perfused sinusoids after LPS injection was increased (7.1-fold) (Fig. 2D). The percentage of non-perfused sinusoids was significantly lowered by OKY-046 (by 61.0%) and S-1452 (by 47.0%), respectively.

OKY-046 decreased the levels of plasma ALT activity at 4 hours after and the levels of plasma TNFα at 1 hour after LPS injection by 22% and 31%, respectively.

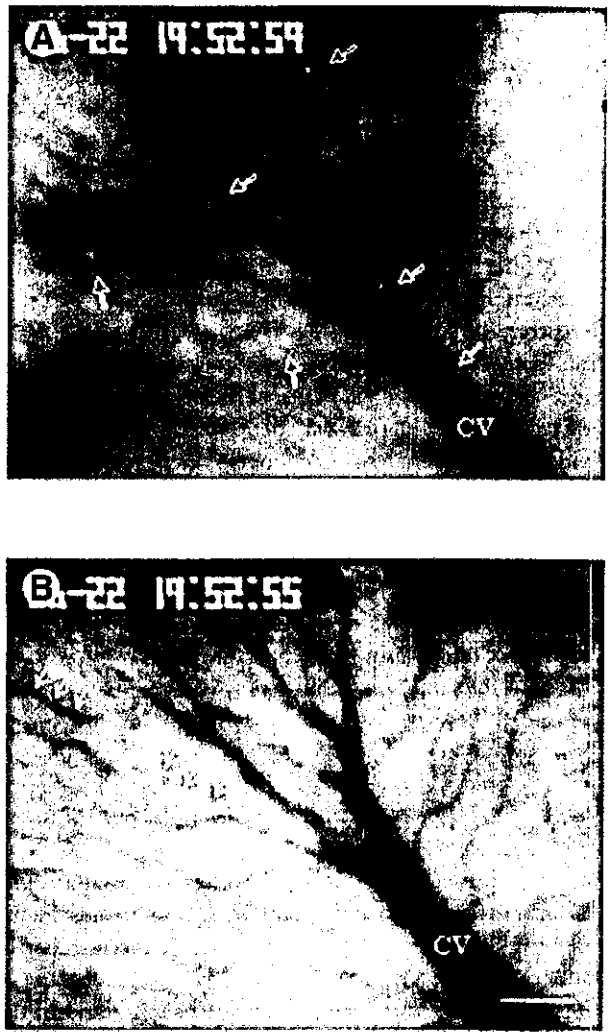

Fig. 1. Representative *in vivo* fluorescence micrographs of the hepatic microcirculation 4 hours after LPS injection. (A) Numerous leukocytes (**open arrows**), which were labeled with rhodamine 6G, adhere to the sinusoids and to the central venules. (B) The sinusoids and hepatic venules were well visualized by the injection of FITC-dextran. The sinusoidal perfusion deficits were detected by direct observation of the microcirculation as evidenced by the cessation of the perfusion (**arrows**) and by the non-visualization of the sinusoids (**arrowheads**). The fluorograph in Fig. 1B shows the same microscopic field as that in Fig. 1A. Bar represents 50 μm.

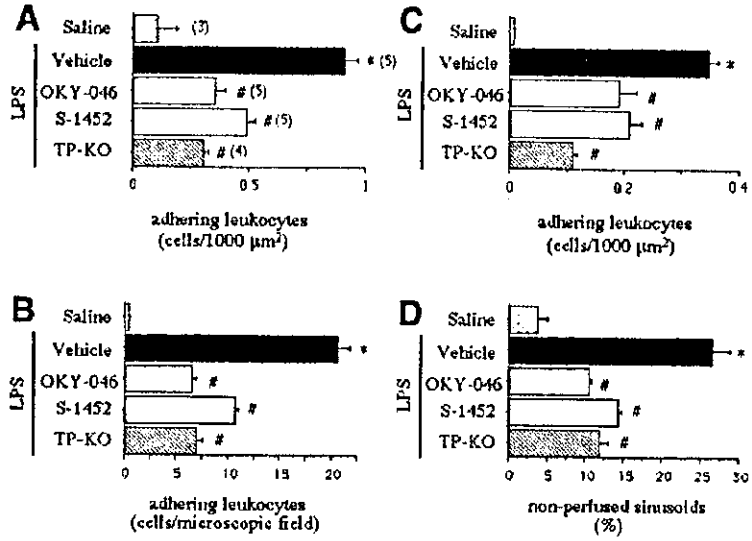

Fig. 2. Effects of LPS on (A) the numbers of leukocytes adhering to the portal venules, (B) the numbers of leukocytes adhering to the sinusoids, (C) the numbers of leukocytes adhering to the central venules, and (D) the percentage of non-perfused sinusoids, all in TP receptor-knockout (KO) mice and in their wild-type counterparts treated with OKY-046 (50 mg/kg, intravenously) and S-1452 (10 mg/kg, p.o.). Numbers in parentheses indicate number of animals. Data are shown as means ± SEM. *$P < .05$ versus Saline-treated mice; #$P < .05$ versus LPS-treated mice.

S-1452 also reduced them by 17% and 40%, respectively (Fig. 3).

To further investigate whether LPS-induced hepatic microcirculatory dysfunction is mediated by endogenously produced TXs, we used TP receptor-knockout mice. As shown in Fig. 2, in wild-type counterparts, LPS caused significant hepatic microcirculatory dysfunction as described above (Figs. 2A–D). In TP receptor-knockout mice, the numbers of leukocytes adhering to the portal venules, sinusoids, and central venules were significantly lower than in wild-type counterparts. Also the percentage of non-perfused sinusoids was lower in TP receptor-knockout mice than in wild-type mice. The levels of ALT and TNFα after LPS administration in TP receptor-knockout mice were decreased by 18% and 28%, respectively (Fig. 3).

Figure 4 illustrates changes in the levels of TXB_2 in the effluent perfusate from isolated perfused liver. The perfusion experiments were performed to determine whether there was a release site of TXA_2 by liver cells. In controls, no significant change in TXB_2 levels appeared (Fig. 4A). Within 15 min of the start of LPS administration, TXB_2 levels were rapidly increased in comparison with the baseline, and then continued to increase (Fig. 4B). Treatment of wild-type mice with OKY-046 completely abolished the increment of TXB_2 in response to LPS (Fig. 4C). In TP receptor-knockout mice, changes in TXB_2 levels after LPS were similar to those in the wild-type counterparts (Fig. 4D). During the perfusion experiment, the perfusion pressure was stable (2~4 cmH_2O) at all time points.

To investigate whether attenuation of hepatic microcirculatory dysfunction by TXA_2 inhibition affected the expression of adhesion molecules, the expression of ICAM-1 and PECAM-1 in the liver was assessed by RT-PCR and by immunohistochemistry (Figs. 5 and 7). LPS resulted in enhanced hepatic expression of messenger RNA (mRNA) of ICAM-1 when compared with that in saline-treated mice (Fig. 5A). OKY-046 partially prevented LPS-induce increase in ICAM-1 mRNA expression. The reduction in ICAM-1 mRNA expression was also seen in TP receptor-knockout mice.

The immunoreactivity with ICAM-1 was demonstrated in the sinusoids of saline-treated mice (Fig. 5B). LPS upregulated ICAM-1 expression in the sinusoids, as well as the hepatic venules (Fig. 5C), and OKY-046 reduced the ICAM-1 immunoreactivity (Fig. 5D).

To examine the significant contribution of ICAM-1 to leukocyte adhesion to the hepatic microvessels, mice were treated with monoclonal antibody against LFA-1, which is a ligand of ICAM-1. As shown in Fig. 6, the anti-LFA-1

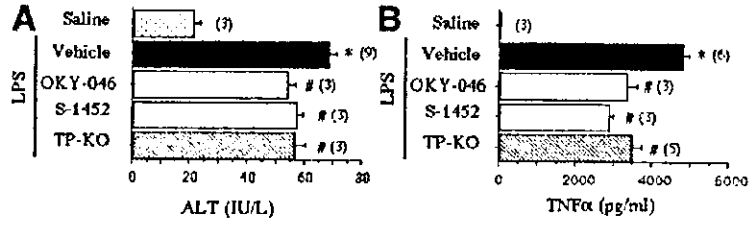

Fig. 3. Effects of LPS on (A) serum ALT activity and (B) the serum concentrations of TNFα in TP receptor-knockout (KO) mice and in their wild-type counterparts treated with OKY-046 (50 mg/kg, intravenously) and S-1452 (10 mg/kg, p.o.). Numbers in parentheses indicate number of animals. Data are shown as means ± SEM. *$P < .05$ versus Saline-treated mice; # $P < .05$ versus LPS-treated mice.

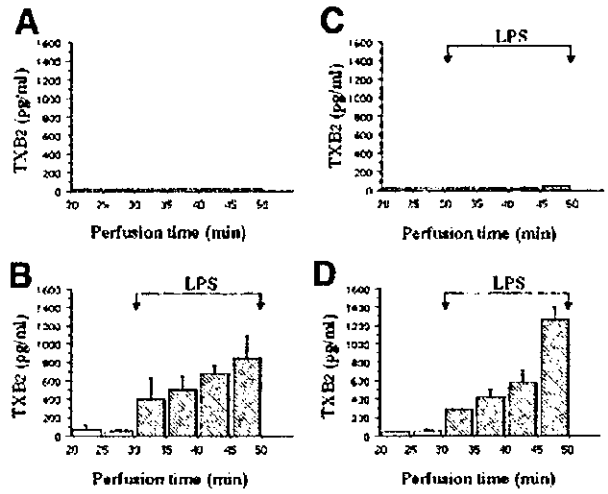

Fig. 4. Changes in the levels of TXB_2 in the effluent perfusate from the isolated perfused livers of wild-type mice (A,B,C) and of TP receptor-knockout mice (D). Livers from LPS-treated wild-type mice (B) and of TP receptor-knockout mice (D). Livers perfused with KH buffer solution alone throughout the experiment served as controls (A). Livers from wild-type mice treated with a combination of OKY-046 (0.05 μg/min for 50 min) and LPS (1.25 μg/min for 20 min) (C). Data are shown as means ± SEM from 3 animals.

antibody minimized hepatic microcirculatory dysfunction in response to LPS.

LPS resulted in slightly enhanced hepatic expression of mRNA of PECAM-1 when compared with that in saline-treated mice, and OKY-046 slightly reduced the expression of PECAM-1 in response to LPS (Fig. 7A). In results of immunohistochemical study, PECAM-1 was demonstrated in saline-treated mice liver (Fig. 7B). LPS enhanced expression of PECAM-1 weakly in comparison with that of ICAM-1 (Fig. 7C). OKY-046 did not affect PECAM-1 expression induced by LPS (Fig. 7D).

Because our results indicate that the hepatic microcirculatory dysfunction is mediated by TXA_2, and because TXA_2 is regulated by COX, we detected the expression of mRNA for COXs using RT-PCR. As shown in Fig. 8, in wild-type counterparts, COX-1 mRNA was expressed in both saline- and LPS-treated livers, whereas the expression of COX-2 mRNA was observed in an LPS-treated liver, but not in a saline-treated liver. The same was true for the livers of TP receptor-knockout mice.

The immunoreactivity with COX-1 in the saline-treated liver (Fig. 9A) and LPS-treated liver (Fig. 9B) was

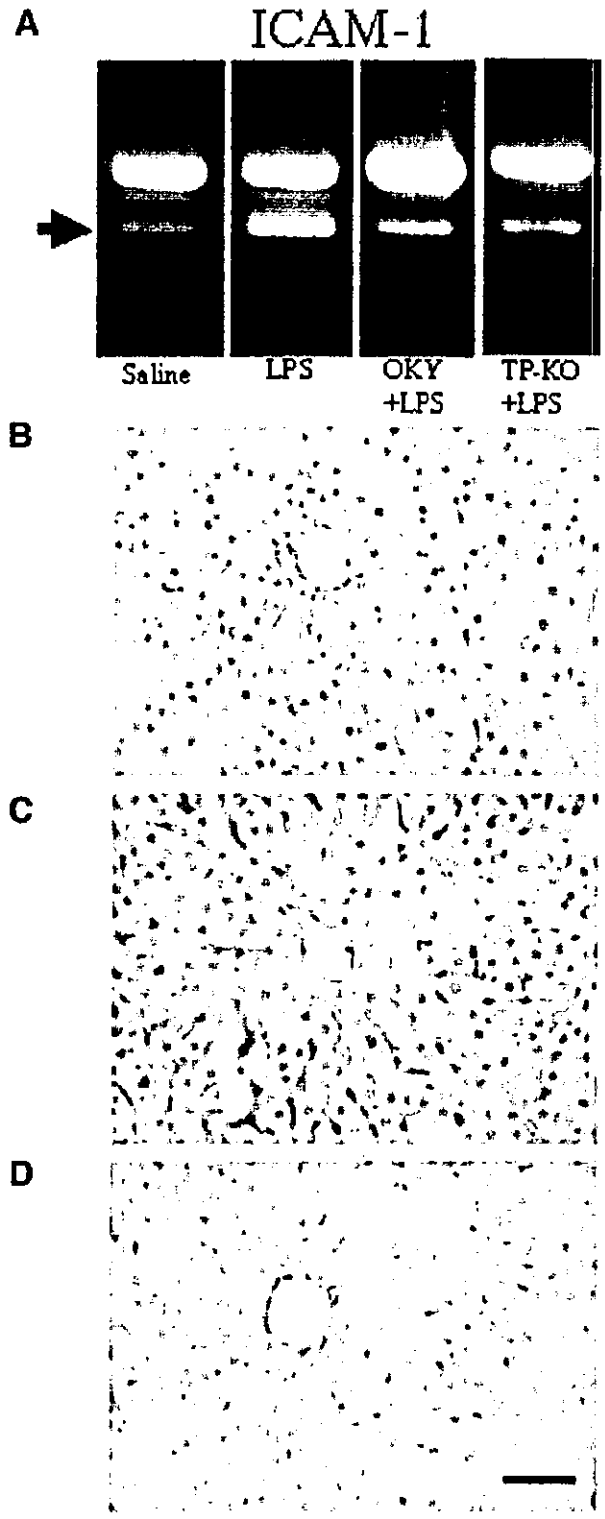

Fig. 5. Hepatic expression of ICAM-1 by RT-PCR analysis (A) and by immunohistochemical staining (B,C,D) 4 hours after LPS administration. LPS enhanced the expression of ICAM-1 mRNA in the liver (A). The hepatic expression of ICAM-1 mRNA after LPS was reduced in mice treated with OKY-046 and in TP- receptor-knockout mice. Immunoreactive ICAM-1 was seen in the sinusoidal lining cells in saline-treated mice (B). LPS enhanced ICAM-1 expression (C), and OKY-046 reduced the expression of ICAM-1 in LPS-treated liver (D). One representative experiment of 2 animals was presented. Bar indicates 50 μm.

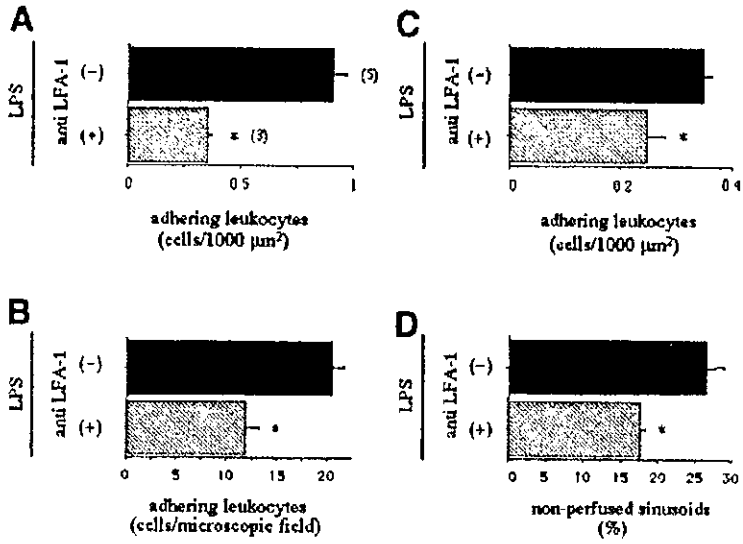

Fig. 6. Effects of an anti-LFA-1 antibody on (A) the numbers of leukocytes adhering to the portal venules, (B) the numbers of leukocytes adhering to the sinusoids, (C) the numbers of leukocytes adhering to the central venules, and (D) the percentage of non-perfused sinusoids at 4 hours after LPS administration. Numbers in parentheses indicate number of animals. Data are shown as means ± SEM. *$P < .05$ versus LPS-treated mice.

detected on the surface of hepatic microvessels. In contrast, the staining of COX-2 was negative in the saline-treated liver (Fig. 9C), however, the immunoreactive COX-2 in the LPS-treated liver was observed on the surface of the sinusoidal lining cells and on the hepatic venules. The most intense staining was shown in the sinusoids (Fig. 9D).

To ascertain which COX isozymes contribute to LPS–induced hepatic microcirculatory dysfunction, mice were pre-treated with SC-560, NS-398, and indomethacin. SC-560, NS-398, and indomethacin significantly lowered the numbers of leukocytes adhering to the portal venules (Fig. 10A), sinusoids (Fig. 10B), and central venules (Fig. 10C), respectively. In sinusoids, indomethacin lowered the numbers of adhered leukocytes more than SC-560 or NS-398 (Fig. 10B). The percentages of non-perfused sinusoids after LPS administration also were lower in mice treated with SC-560, NS-398, or indomethacin than in mice treated with vehicle (Fig. 10D). SC-560, NS-398, and indomethacin themselves did not significantly change leukocyte adhesion and sinusoidal perfusion in saline-treated mice (data not shown).

Four hours after LPS injection, the levels of ALT were significantly increased (3.2-fold) in comparison with the saline-treated controls (Fig. 11A). SC-560, NS-398, and indomethacin significantly decreased ALT levels after LPS injection by 35.0%, 42.0%, and 42.0%, respectively. The levels of TNFα 1 hour after LPS injection were significantly increased (Fig. 11B). SC-560, NS-398, and indomethacin significantly decreased TNFα levels, by 49.0%, 30.0%, and 33.0%, respectively.

Discussion

The results of the present study showed that OKY-046, a TXA_2 synthase inhibitor and S-1452, a TXA_2 receptor antagonist attenuated LPS-induced hepatic microcirculatory dysfunction as indicated by an increase of leukocytes adhering to the hepatic microvessels, as well as by impaired sinusoidal perfusion. To rule out the possibility that LPS affects the systemic hemodynamics, we measured the arterial blood pressure. The administration of LPS at a dose of 0.3 mg/kg (intravenously) did not reduce the mean arterial blood pressure. The hepatic microcirculatory dysfunction in response to LPS was accompanied by decreases in the serum levels of ALT and TNFα. These results suggest that TXA_2 enhances hepatic microcirculatory dysfunction during endotoxemia. This possibility was supported by our finding that TP receptor-knockout mice minimized liver injury and hepatic microcirculatory dysfunction in response to LPS by inhibiting TNFα production.

The finding that TXA_2 appears to modulate TNFα production after LPS administration (Fig. 3) is consistent with the findings of others,[7,27,28] that TXA_2 synthase inhibitor and TXA_2 receptor antagonist suppress LPS-induced TNFα release from macrophages[7,27] and from the perfused heart.[28] The inhibitory effects of OKY-046 and S-1452 on TNFα production in response to LPS were partial (30–40% reduction), while OKY-046 completely inhibited TXB_2 release in perfusate from the LPS-treated liver. These results suggest that other factors may be involved in the regulation of TNFα generation.

We observed that OKY-046 prevented the LPS-induced increase in ICAM-1 expression in the intrahepatic

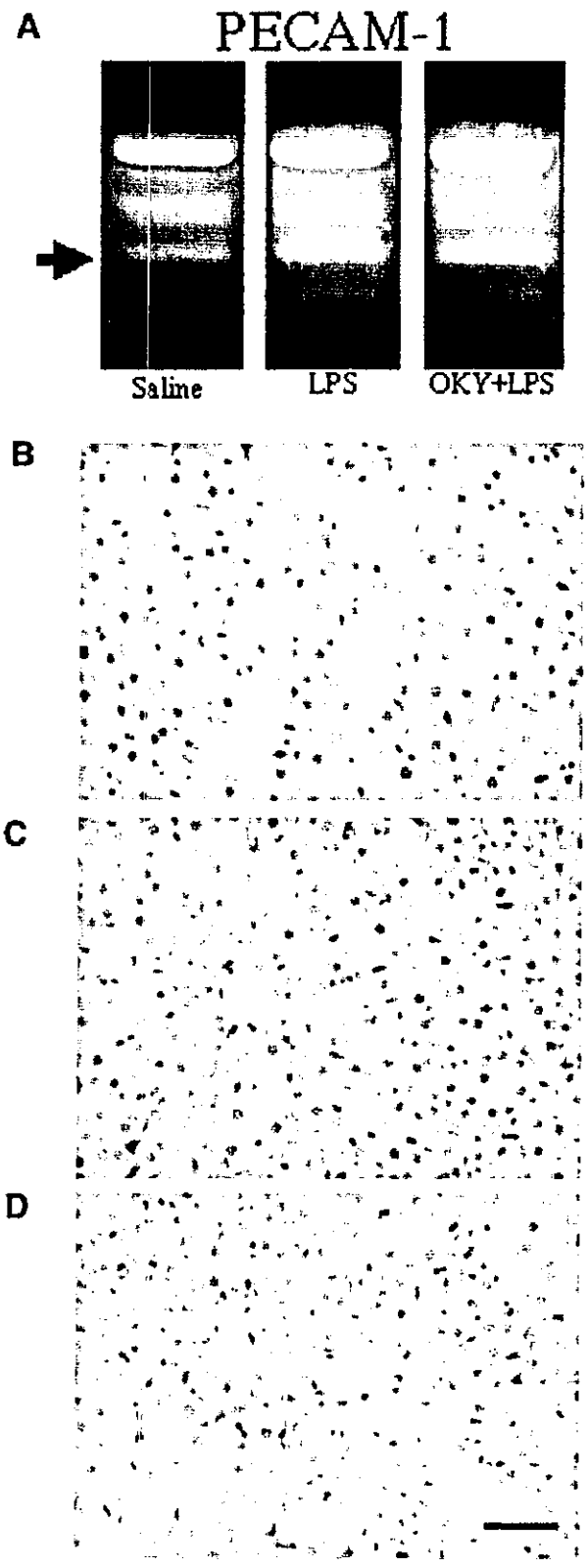

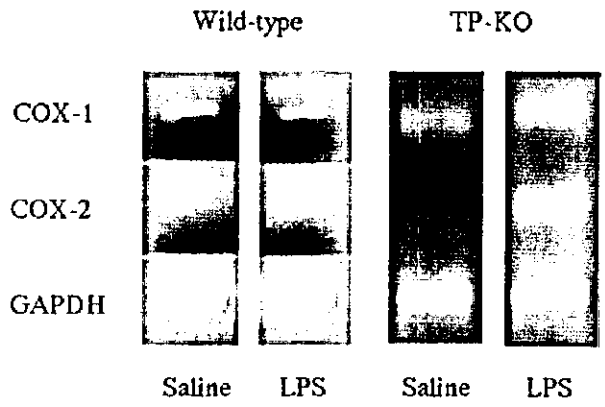

Fig. 8. Expression of COXs in liver tissue by RT-PCR analysis. Liver tissue was excised 4 hours after saline or LPS administration in wild-type and TP receptor-knockout (KO) mice. One representative experiment of 2 animals were presented.

circulation, and that TP-receptor knockout mice exhibited decreased expression of ICAM-1 in the LPS-treated liver (Fig. 5). It has been reported that TXA_2 receptor antagonist suppresses the expression of ICAM-1 on human umbilical vein endothelial cells.[29] These findings suggest that increased ICAM-1 expression mediated by TP-receptor signaling may have facilitated leukocyte adhesion in the liver during endotoxemia. However, it is well known that TNFα released from Kupffer cells in response to LPS induces the transcriptional activation of ICAM-1 expression on the hepatic microvessels independently through TXA_2 signaling,[30] and that TNFα is the central mediator responsible for upregulation of hepatic ICAM-1 expression in response to hepatotoxicants such as carbon tetrachloride[31] and endotoxin.[32]

Enhanced ICAM-1 expression in the liver has been shown to contribute to leukocyte adhesion to the hepatic venules as well as to the sinusoids.[30] Our findings that the anti-LFA-1 antibody attenuated leukocyte adhesion indicates that ICAM-1 is involved in leukocyte adhesion in the endotoxemic liver. These results also suggest that attenuation of hepatic microcirculatory dysfunction is attributable to the reduction of ICAM-1 expression by

Fig. 7. Expression and immunoreactivity of PECAM-1 in liver tissue by RT-PCR analysis (A) and immunohistochemical staining (B,C,D) in liver tissue from mice treated with saline, LPS, and OKY-046/LPS. LPS resulted in slightly enhanced hepatic expression of mRNA of PECAM-1 when compared with that in saline-treated mice, and OKY-046 slightly reduced the expression of PECAM-1 in response to LPS (Fig. 7A). The immunoreactivity with PECAM-1 in saline-treated liver was weak (B), and was slightly enhanced in LPS-treated liver (C). OKY-046 did not change significantly the expression of PECAM-1 in LPS-treated liver (D). Liver tissue was excised 4 hours after LPS administration. One representative experiment of 2 animals was presented. Bar indicates 50 μm.

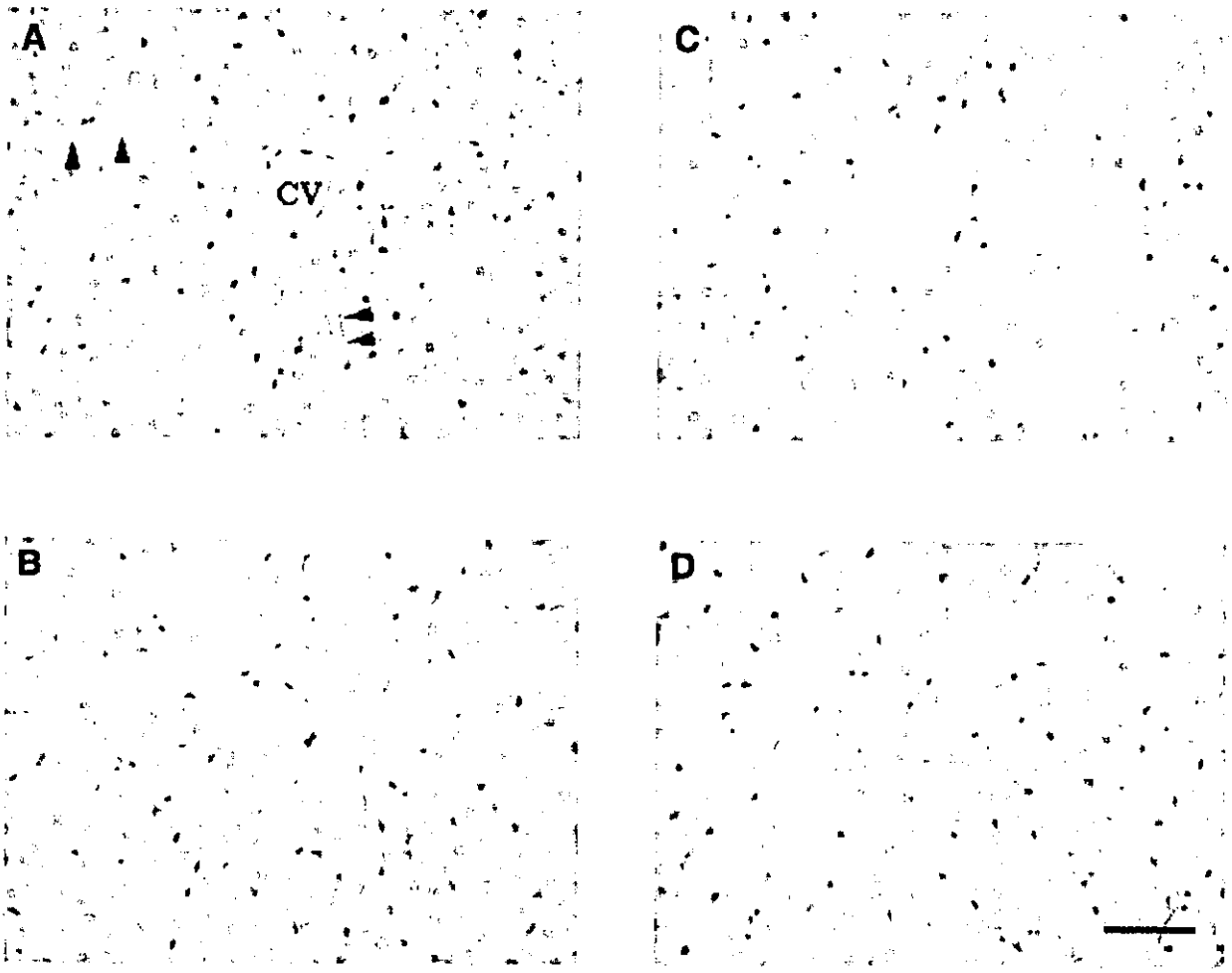

Fig. 9. Immunohistochemical localization of COX-1 (A,B) and COX-2 (C,D) in liver tissue 4 hours after the administration of saline or LPS. Immunoreactive COX-1 was seen in the sinusoidal lining cells in both saline- (A) and LPS-treated mice (B). On the other hand, the immunoreactivity with COX-2 was negative in saline-treated animals (C), whereas it was enhanced in the sinusoids after LPS treatment (D). One representative experiment of 2 animals were presented. Bar indicates 50 μm.

TXA_2 inhibition. However, others[33] have reported that ICAM-1 is involved in accumulation of leukocytes in the hepatic venules, but not in the sinusoids. Furthermore, the present study showed that OKY-046 did not significantly change the LPS-induced increase in the expression of PECAM-1, suggesting that microcirculatory dysfunction improved by TXA_2 inhibition is independent of PECAM-1 expression, and this is consistent with the findings of others.[33]

LPS administration to the isolated perfused liver resulted in a rapid and significant release of TXB_2 into the perfusate, suggesting that the liver is an important source of TXA_2, and that TXA_2 seems to be an inflammatory mediator in the early phase of endotoxemia. We measured the levels of TXB_2 in the effluent perfusate because the levels of TXs and PGs were artificially elevated with ease by mechanical stimulation.[20] In the liver, in response to LPS, TXA_2 is released from nonparenchymal cells (*i.e.*, Kupffer cells[6] and sinusoidal endothelial cells).[34] Of these, Kupffer cells are a major source of TXA_2. However, the possibility that activated platelets are productive sources of TXA_2 *in vivo* cannot be excluded.

To explore whether COX-1 and COX-2 activities are involved in hepatic microcirculatory dysfunction during endotoxemia, mice were treated with the selective COX-1 inhibitor SC-560 and the selective COX-2 inhibitor NS-398. Both SC-560 and NS-398 significantly reduced liver injury and hepatic microcirculatory dysfunction in response to LPS. These results suggest that COX-1 and COX-2 are involved in liver injury. In fact, the levels of ALT activity after LPS combination with galactosamine were significantly decreased in COX-2-deficient mice.[12] A selective COX-2 inhibitor, FK3311, limited liver injury in dogs caused by ischemia/reperfusion and restored he-

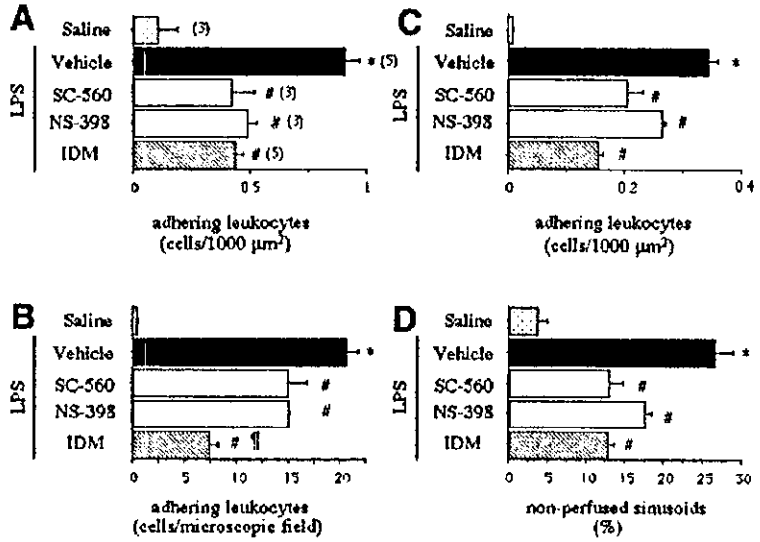

Fig. 10. Effects of SC-560 (10 mg/kg, p.o.), NS-398 (10 mg/kg, s.c.), and indomethacin (IDM) on (A) the numbers of leukocytes adhering to the portal venules, (B) the numbers of leukocytes adhering to the sinusoids, (C) the numbers of leukocytes adhering to the central venules, and (D) the percentage of non-perfused sinusoids after LPS administration. The numbers of adhering leukocytes and of sinusoids were determined 4 hours after LPS injection. Numbers in parentheses indicate number of animals. Data are shown as means ± SEM. *$P < .05$ versus Saline-treated mice; #$P < .05$ versus LPS-treated mice; ¶$P < .05$ versus NS-398-treated mice and SC-560-treated mice.

patic tissue blood flow.[13] Inhibition of COX-2 with NS-398 improved survival from sepsis induced by cecal ligation and puncture in mice.[35] In contrast, Leach et al.[36] reported that inhibition of COX-2 with NS-398 failed to attenuate liver injury elicited by LPS in rats. The reasons for these discrepancies remain unclear, though they may be caused by differences in the animals and the doses of drugs used.

The contribution of PGs generated through the action of COX-1 to hepatic microcirculatory dysfunction and leukocyte adhesion can be estimated from the reduction in the leukocyte adhesion variables after the administration of a COX-1 selective inhibitor, SC-560. This agent used in the present experimental conditions exhibits good selectivity to COX-1. The same was also true in the case of COX-2 inhibition using the COX-2 inhibitor NS-398. In the portal venules, the adhesion of leukocytes were reduced equally by SC-560 and NS-398. This indicates that the PGs generated through COX-1 and COX-2 enhanced the adhesion equally. But, indomethacin did not inhibit the adhesion more intensely than SC-560 and NS-398 in portal venules in the present experiment, although this inhibitor blocks both COX-1 and COX-2. We supposed that there might be a threshold concentration of TXA_2 generated in the microvasculature to induce leukocyte adhesion. Without treatment with COX inhibitors, the amount of TXA_2 generated may be more than the threshold concentration of TXA_2 when either COX-1 or COX-2 is inhibited. If PGs are generated through the action of COX-1 and COX-2, and if no alternative pathway for PG generation is present, the inhibition of either COX-1 or COX-2, or both, certainly reduces the PG levels, which may be lower than the threshold concentration. If the inhibition of either COX-1 or COX-2 is enough to lower the TXA_2 levels below the threshold concentration, the effects of indomethacin are not different from those observed under the inhibition of COX-1 or COX-2. Judging from the results of the perfusion experiment, sites of TXA_2 generation were certainly present in the liver. So, the concentration of TXA_2 may be higher in the sinusoids or in the central venules than in the portal venules. TXA_2 at a concentration over the threshold concentration may induce adhesion in a concentration-dependent manner. In fact, we can observe the effects of indomethacin to be the sum of the inhibition of COX-1 and that of COX-2 in the sinusoids or central venules, where the TXA_2 concentration may be higher than that in portal venules.

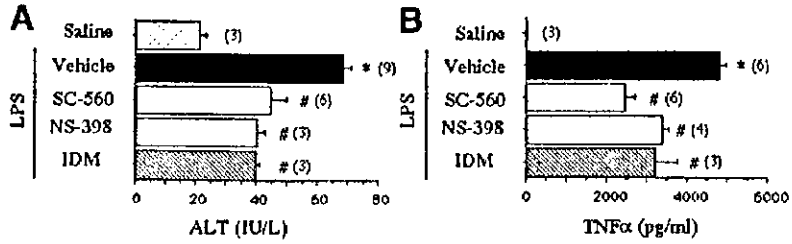

Fig. 11. Effects of SC-560 (10 mg/kg, p.o.), NS-398 (10 mg/kg, s.c.), and indomethacin (IDM 10 mg/kg, p.o.) on (A) serum ALT activity and (B) the serum concentrations of TNFα after LPS administration. Numbers in parentheses indicate number of animals. Data are shown as means ± SEM. *$P < .05$ versus Saline-treated mice; #$P < .05$ versus LPS-treated mice.

In conclusion, our present study clarifies the important role played by TXA_2 in hepatic microcirculatory dysfunction elicited by LPS administration, although factors other than TXA_2 were reported previously.[37–42] LPS-induced hepatic microcirculatory dysfunction was associated with TXA_2 generation in the liver. The inhibitory effects of TXA_2 synthase inhibitor and TXA_2 receptor antagonist on the hepatic response to LPS were similar to the effects of selective COX-1 and COX-2 inhibitors, suggesting that endogenous TXA_2 derived from both COX-1 and COX-2 participate in LPS-induced liver injury by enhancement of TNFα production. TP receptor signaling may be related to the upregulation of expression of an adhesion molecule, ICAM-1.

Acknowledgment: The authors thank Michiko Ogino and Osamu Katsumata for their technical assistance. The authors also express their thanks to C.W.P. Reynolds for correcting the English of this manuscript.

References

1. McCuskey RS. Hepatic microvascular response to endotoxemia and sepsis. In: Messmer K, Menger MD, eds. Progress in Applied Microcirculation. Basel: Karger, 1993;19:76–84.
2. Vollmar B, Rüttinger D, Wanner GA, Leiderer R, Menger MD. Modulation of Kupffer cell activity by gadolinium chloride in endotoxemic rats. Shock 1996;6:434–441.
3. Chensue SW, Terebuh PD, Remick DG, Scales WE, Kunkel SL. In vivo biologic and immunohistochemical analysis of interleukin-1 alpha, beta and tumor necrosis factor during experimental endotoxemia. Kinetics, Kupffer cell expression, and glucocorticoid effects. Am J Pathol 1991;138: 395–402.
4. Luster MI, Germolec DR, Yoshida T, Kayama F, Thompson M. Endotoxin-induced cytokine gene expression and excretion in the liver. HEPATOLOGY 1994;19:480–488.
5. Matsumoto Y, Ito Y, Hayashi I, Majima M, Ishii K, Katagiri H, Kakita A. Effect of FR167653, a novel inhibitor of tumor necrosis factor alpha and interleukin-1 beta synthesis on lipopolysaccharide-induced hepatic microvascular dysfunction in mice. Shock 2002;17:411–415.
6. Decker K. Biologically active products of stimulated liver macrophages. Eur J Biochem 1990;192:245–361.
7. Altavilla D Squadrito F, Canale P, Ioculano M, Squadrito G, Campo GM, Serrano M, et al. G619, a dual thromboxane synthase inhibitor and thromboxane A_2 receptor antagonist, inhibits tumor necrosis factor-α biosynthesis. Eur J Pharmacol 1995;286:31–39.
8. Ishiguro S, Arii S, Monden K, Adachi Y, Funaki N, Higashitsuji H, Fujita S, et al. Identification of the thromboxane A_2 receptor in hepatic sinusoidal endothelial cells and its role in endotoxin-induced liver injury in rats. HEPATOLOGY 1994;20:1281–1286.
9. Karck U, Peters T, Decker K. The release of tumor necrosis factor from endotoxin-stimulated rat Kupffer cells is regulated by prostaglandin E_2 and dexamethasone. J Hepatol 1988;7:352–361.
10. Otto JC, Smith WL. Prostaglandin endoperoxide synthases-1 and -2. J Lipid Mediat Cell Signal 1995;12:139–156.
11. Ruetten H, Thiemermann C. Effect of calpain inhibitor I, an inhibitor of the proteolysis of IκB, on the circulatory failure and multiple organ dysfunction caused by endotoxin in the rat. Br J Pharmacol 1997;121:695–704.
12. Dinchuk JR, Car BD, Focht RJ, Johnson JJ, Jaffee BD, Covington MB, Contel NR, et al. Renal abnormalities and an altered inflammatory response in mice lacking cyclooxygenase II. Nature 1995;378:406–409.
13. Sunose Y, Takeyoshi I, Ohwada S, Tsutsumi H, Iwazaki S, Kawata K, Kawashima Y, et al. The effect of cyclooxygenase-2 inhibitor FK3311 on ischemia-reperfusion injury in a canine total hepatic vascular exclusion model. J Am Coll Surg 2001;192:54–62.
14. Hanasaki K, Nagasaki T, Arita H. Characterization of platelet thromboxane A_2/prostaglandin H_2 receptor by a novel thromboxane receptor antagonist, [3H]S-145. Biochem Pharmacol 1989;38:2007–2017.
15. Smith CJ, Zhang Y, Koboldt CM, Muhammad J, Zweifel BS, Shaffer A, Talley JJ, et al. Pharmacological analysis of cyclooxygenase-1 in inflammation. Proc Natl Acad Sci U S A 1998;95:13313–13318.
16. Futaki N, Yoshikawa K, Hamasuka Y, Arai I, Higuchi S, Iizuka H, Otomo S. NS-398, a novel non-steroidal anti-inflammatory drug with potent analgesic and antipyretic effects, which causes minimal stomach lesions. Gen Pharmacol 1993;24:105–110.
17. Xiao CY, Hara A, Yuhki K, Fujino T, Ma H, Okada Y, Takahata O, et al. Roles of prostaglandin I2 and thromboxane A2 in cardiac ischemia-reperfusion injury. Circulation 2001;104:2210–2205.
18. Post S, Palma P, Rentsch M, Gonzalez MD, Menger MD. Hepatic reperfusion injury following cold ischemia in the rat: potentials and quantitative analysis by in vivo fluorescence microscopy. In: Messmer K, Menger MD, eds. Progress in Applied Microcirculation. Basel: Karger, 1993;19:152–166.
19. Suematsu M, Goda N, Sano T, Kashiwagi S, Shinoda Y, Ishimura Y. Carbon monoxide: an endogenous modulator of sinusoidal tone in the perfused rat liver. J Clin Invest 1995;96:2431–2437.
20. Suzuki Y, Ueno A, Kawamura M, Nishiyama K, Katori M, Okabe H. Prostaglandin levels in the rat resting gastric wall and enhancement of prostaglandin E_2 generation after administration of mild hyperosmotic saline solution into the gastric lumen. Eicosanoids 1990;3:23–27.
21. Boku K, Ohno T, Saeki T, Hayashi H, Hayashi I, Katori M, Murata T, et al. Adaptive cytoprotection mediated by prostaglandin I_2 is attributable to sensitization of CGRP-containing sensory nerves. Gastroenterology 2001; 120:134–143.
22. Majima M, Isono M, Ikeda Y, Hayashi I, Hatanaka K, Harada Y, Katsumata O, et al. Significant roles of inducible cyclooxygenase (COX)-2 in angiogenesis in rat sponge implants. Jpn J Pharmacol 1997;75:105–114.
23. Molle WV, Berghe JV, Brouchaert P, Libert C. Tumor necrosis factor-α-induced lethal hepatitis: pharmacological intervention with verapamil, tannic acid, picotamide and K76COOH. FEBS Lett 2000;467:201–205.
24. Shirabe K, Kin S, Shinagawa Y, Chen S, Payne WD, Sugimachi K. Inhibition of thromboxane A_2 activity during warm ischemia of the liver. J Surg Res 1996;61:103–107.
25. Sugawara Y, Harihara Y, Takayama T, Makuuchi M. Suppression of cytokine production by thromboxane A_2 inhibitor in liver ischemia. Hepatogastroenterology 1998;45:1781–1786.
26. Nagai H, Shimazawa T, Yakuo I, Aoki M, Kosa A, Kasahara M. The role of thromboxane A_2 (TXA_2) in liver injury in mice. Prostaglandins 1989; 38:439–446.
27. Kuhn DC, Stauffer JL, Gaydos LJ, Lacey SL, Demers LM. An inhibitor of thromboxane production attenuates tumor necrosis factor release by activated human alveolar macrophages. Prostaglandins 1993;46:195–205.
28. Grandel U, Fink L, Blum A, Heep M, Buerke M, Kraemer H-J, Mayer K, et al. Endotoxin-induced myocardial tumor necrosis factor-α synthesis depresses contractility of isolated rat hearts. Evidence for a role of sphingosine and cyclooxygenase-2-derived thromboxane production. Circulation 2000;102:2758–2764.
29. Ishizuka T, Kawakami M, Hidaka T, Matsuki Y, Takamizawa M, Suzuki K, Kurita A, et al. Stimulation with thromboxane A_2 (TXA_2) receptor agonist enhances ICAM-1, VCAM-1 or ELAM-1 expression by human vascular endothelial cells. Clin Exp Immunol 1998;112:464–470.
30. Sakamoto S, Okanoue T, Itoh Y, Nakagawa Y, Nakamura H, Morita A, Daimon Y, et al. Involvement of Kupffer cells in the interaction between neutrophils and sinusoidal endothelial cells in rats. Shock 2002;18:152–157.
31. Neubauer K, Ritzel A, Saile B, Ramadori G. Decrease of platelet-endothelial cell adhesion molecule 1-gene-expression in inflammatory cells and in endothelial cells in the rat liver following CCl(4)-administration and in vitro after treatment with TNFalpha. Immunol Lett 2000;74:153–164.

32. Essani NA, Fisher MA, Farhood A, Manning AM, Smith CW, Jaeschke H. Cytokine-induced upregulation of hepatic intercellular adhesion molecule-1 messenger RNA expression and its role in the pathophysiology of murine endotoxin shock and acute liver failure. HEPATOLOGY 1995;21:1632–1639.
33. Chosay JG, Fisher MA, Farhood A, Ready KA, Dunn CJ, Jaeschke H. Role of PECAM-1 (CD31) in neutrophil transmigration in murine models of liver and peritoneal inflammation. Am J Physiol 1998;274: G776–G782.
34. Rieder H, Ramadori G, Allmann K-H, Meyer K-H, Büschenfelde M. Prostanoid release of cultured liver sinusoidal endothelial cells in response to endotoxin and tumor necrosis factor. J Hepatol 1990;11:359–366.
35. Mack Strong VE, Mackrell PJ, Concannon EM, Mestre JR, Smyth GP, Schaefer PA, Stapleton PP, et al. NS-398 treatment after trauma modifies NF-κB activation and improves survival. J Surg Res 2001;98,40–46.
36. Leach M, Hamilton LC, Olbrich A, Wray GM, Thiemermann C. Effects of inhibitors of the activity of cydo-oxygenase-2 on the hypotension and multiple organ dysfunction caused by endotoxin: a comparison with dexamethasone. Br J Pharmacol 1998;124:586–592.
37. Doi F, Goya T, Torisu M. Potential role of hepatic macrophages in neutrophil-mediated liver injury in rats with sepsis. HEPATOLOGY 1993;17:1086–1094.
38. Shiratori Y, Tanaka M, Hai K, Kawase T, Shirna S, Sugimoto T. Role of endotoxin-responsive macrophages in hepatic injury. HEPATOLOGY 1990; 11:183–192.
39. Dahm LJ, Schultze AE, Roth RA. Activated neutrophils injure the isolated, perfused rat liver by an oxygen radical-dependent mechanism. Am J Pathol 1991;139:1009–1020.
40. Kurose I, Kato S, Ishii H, Fukumura D, Miura S, Suematsu M, Tsuchiya M. Nitric oxide mediates lipopolysaccharide-induced alteration of mitochondrial function in cultured hepatocytes and isolated perfused liver. HEPATOLOGY 1993;18:380–388.
41. Sakaguchi T, Nakamura S, Suzuki S, Oda T, Ichiyama A, Baba S, Okamoto T. Participation of platelet-activating factor in the lipopolysaccharide-induced liver injury in partially hepatectomized rats. HEPATOLOGY 1999;30:959–967.
42. Feder LS, Todaro JA, Laskin DL. Characterization of interleukin-1 and interleukin-6 production by hepatic endothelial cells and macrophages. J Leukocyte Biol 1993;53:126–132.

GASTROENTEROLOGY 2004;126:873–885

Pioglitazone Prevents Alcohol-Induced Fatty Liver in Rats Through Up-regulation of c-Met

KENGO TOMITA,* TOSHIFUMI AZUMA,* NAOTO KITAMURA,* JIRO NISHIDA,† GEN TAMIYA,§ AKIRA OKA,§ SAYAKA INOKUCHI,* TAKESHI NISHIMURA,* MAKOTO SUEMATSU,‖ and HIROMASA ISHII*

Departments of *Internal Medicine and ‖Biochemistry, Keio University School of Medicine, Tokyo, Japan; †Department of Gastroenterology, Ichikawa General Hospital, Tokyo Dental College, Chiba, Japan; and §Department of Molecular Life Science, School of Medicine, Tokai University, Kanagawa, Japan

Background & Aims: Treatment of steatosis is important in preventing development of fibrosis in alcoholic liver diseases. This study aimed to examine if pioglitazone, an antidiabetic reagent serving as a ligand of peroxisome proliferator-activated receptor gamma (PPARγ), could prevent alcoholic fatty liver. *Methods:* Rats fed with an ethanol-containing liquid diet were given the reagent at 10 mg/kg per day intragastrically for 6 weeks. Hepatic genes involved in actions of the reagent were mined by transcriptome analyses, and their changes were confirmed by real-time polymerase chain reaction and Western blotting analyses. The direct effects of pioglitazone on primary-cultured hepatocytes were also assessed in vitro. *Results:* Pioglitazone significantly attenuated steatosis and lipid peroxidation elicited by chronic ethanol exposure without altering insulin resistance. Mechanisms for improving effects of the reagent appeared to involve restoration of the ethanol-induced down-regulation of c-Met and up-regulation of stearoyl-CoA desaturase (SCD). Such effects of pioglitazone on the c-Met signaling pathway resulted from its tyrosine phosphorylation and resultant up-regulation of the apolipoprotein B (apoB)-mediated lipid mobilization from hepatocytes through very low–density lipoprotein (VLDL) as well as down-regulation of sterol regulatory element binding protein (SREBP)-1c and SCD levels and a decrease in triglyceride synthesis in the liver. *Conclusions:* Pioglitazone activates c-Met and VLDL-dependent lipid retrieval and suppresses triglyceride synthesis and thereby serves as a potentially useful stratagem to attenuate ethanol-induced hepatic steatosis.

Chronic consumption of excess alcohol is hepatotoxic in humans and produces an accumulation of hepatic triglycerides to cause steatosis. These changes are pathologically characterized by macrovesicular fatty degeneration and occur in pericentral regions. Recent clinical studies provided evidence that such an accumulation of triglycerides in the liver is not benign but could lead to fibrosis and cirrhosis with effective treatment remaining to be established.[1,2] Because the hepatic steatosis often coincides with hyperinsulinemia and insulin resistance, treatment that renders patients sensitive to the hormone could be beneficial. Such a possibility was well supported by previous studies showing that metformin, an agent improving insulin resistance of the liver, improved steatosis, hepatomegaly, and the release of transaminases in insulin-resistant ob/ob mice with nonalcoholic fatty liver; mechanisms for such beneficial effects of metformin appear to involve down-regulation of tumor necrosis factor-α (TNF-α) and TNF-inducible genes such as SREBP-1 and uncoupling protein-2[3] as well as increased phosphorylation and activation of AMP-activated protein kinase (AMPK).[4] The fact that the histological features and natural history of alcoholic fatty liver are similar to those of nonalcoholic fatty liver suggests that unidentified common mechanisms for pathogenesis of hepatic steatosis could be involved in these 2 disease conditions. However, utilization of metformin is unlikely to be applicable to treat alcoholic steatosis because of its side effect of lactic acidosis, an important complication of clinical alcoholic liver injury.

Such circumstances led us to examine if another class of antidiabetic agents such as thiazolidinediones are effective to treat hepatic steatosis caused by chronic ethanol administration. These reagents are ligands of perox-

Abbreviations used in this paper: ALT, alanine aminotransferase; AMPK, AMP-activated protein kinase; apoB, apolipoprotein B; AST, aspartate aminotransferase; BADGE, bisphenol A diglycidyl ether; HGF, hepatocyte growth factor; 4-HNE, 4-hydroxynonenal; HOX, heme oxygenase; GAPDH, glyceraldehyde-3-phosphate dehydrogenase; PPAR, peroxisome proliferator-activated receptor; PCR, reverse-transcriptase polymerase chain reaction; TG, triglyceride; TNF-α, tumor necrosis factor-α; VLDL, very low-density lipoprotein; ZDF fa/fa, Zucker diabetic fatty.

0016-5085/04/$30.00
doi:10.1053/j.gastro.2003.12.008

isome proliferator-activated receptor γ (PPARγ), which is expressed at high levels in adipocytes, forms a heterodimeric DNA-binding complex with retinoid X receptor, and acts as a transcriptional regulator of genes involved in adipocyte lipid metabolism. One such reagent, troglitazone, was reported to reduce the excessive islet triglyceride (TG) content of Zucker diabetic fatty (ZDF fa/fa) rats, which led to the restoration of β-cell function and the prevention of lipoapoptosis of β cells.[5,6] Troglitazone has also been shown to reduce TG content in liver and heart of prediabetic ZDF rats[6] or to reduce hepatic TG contents concurrently with improvement of plasma levels of TG and insulin in ZDF fa/fa rats suggesting restoration of SREBP-1 gene expression.[7] To examine effectiveness of thiazolidinediones on the experimental hepatic steatosis caused by chronic ethanol administration, we have herein chosen pioglitazone, another derivative of the antidiabetic reagents; this compound has never been reported so far to cause lactic acidosis or to increase transaminases, whereas troglitazone was withdrawn from the market after a case report of severe hepatic failure.[8] Our attempt to examine the hypothesis in this study has not only shown the effectiveness of pioglitazone but also shed light on significance of the c-Met–mediated signaling pathway to regulate synthesis and removal of triglycerides as a potential therapeutic target for treatment of ethanol-induced hepatic steatosis and injury.

Materials and Methods

Animal Feeding

The Lieber–DeCarli diets were purchased from Bio-Serv, Inc (Frenchtown, NJ).[9] Four-week-old male Sprague–Dawley rats housed in temperature- and light-controlled rooms were randomly divided into 3 groups: (A) rats fed ethanol-containing liquid diet for 6 weeks (n = 9), (B) rats pair fed ethanol-containing liquid diet for 6 weeks during which they were given pioglitazone (10 mg/kg body weight per day) once every 24 hours intragastrically (n = 9), and (C) rats pair fed isocaloric liquid diet without ethanol for 6 weeks (n = 9). Pioglitazone was dissolved in methylcellulose before use. Maeshida et al.[10] reported that pioglitazone was well absorbed from the gastrointestinal tract at an extent of 96% in rats. The plasma concentration of pioglitazone peaked at 4 hours after dosing and declined with a half-life of 2.6 hours. They also showed the concentration of radioactivity in rat tissues at 0.5, 2, 6, 10, 24, and 72 hours after oral administration of [^{14}C]pioglitazone.[10] The radioactivity of liver tissue was higher than that of plasma, and it peaked at 6 hours. The concentration of pioglitazone in liver at 24 hours after oral administration is still about one third of the concentration at 30 minutes. There is another report describing that 1 dose of 10 mg/kg of pioglitazone every 24 hours ameliorated insulin resistance associated with diabetes in rats.[11] Based on these previous papers, we think it reasonable to expect that 1 dose of 10 mg/kg of pioglitazone every 24 hours is sufficient to sustain effective concentration. The rats in groups A and C were given methylcellulose once every 24 hours intragastrically for 6 weeks in the same amount as their corresponding litter mates in group B. The rats in group B and group C were pair fed daily on an isoenergetic basis with the corresponding litter mates fed the ethanol-containing diet (group A). To investigate whether another thiazolidinedione, troglitazone, could prevent alcoholic fatty liver, we next gave troglitazone (200 mg/kg body weight/day) to 8-week-old male SD rats (n = 6), instead of pioglitazone, in the same way as our last examination of pioglitazone. Troglitazone was also well absorbed from the gastrointestinal tract, and the highest uptake by the liver was shown in rats.[12] All animals received humane care in compliance with the National Research Council's criteria outlined in the "Guide for the Care and Use of Laboratory Animals" prepared by the U.S. National Academy of Sciences and published by the U.S. National Institutes of Health.

Biochemical and Histological Analysis

Hepatic triglyceride contents were measured as previously described.[13] For histological analysis, liver tissue was fixed in 4% paraformaldehyde and embedded in paraffin. Alternatively, hepatic lipids were stained by an oil red O method (Nacalai Tesque Inc., Kyoto, Japan). For protein or RNA analysis, tissue was frozen in liquid nitrogen and stored at −80°C until used. Apoptosis was analyzed with TUNEL staining (Apoptosis Detection System, Promega Corp., Madison, WI) according to the manufacturer's instructions. At least 2 individual livers were examined in each group by counting the density of the positive-staining hepatocytes in 5 random × 200 fields/liver. Serum concentrations of alanine aminotransferase (ALT), aspartate aminotransferase (AST), triglyceride, total cholesterol, phospholipids, total proteins, albumin, and free fatty acids were measured with a standard clinical autoanalyzer (Hitachi 7170; Hitachi Ltd., Tokyo, Japan). Plasma glucose was measured by the glucose oxidase method with a glucose analyzer II (Beckman Instruments, Brea, CA). Plasma TG levels were measured with a GPO-Trinder triglyceride kit (Sigma, St. Louis, MO). Plasma leptin and insulin were assayed with Linco leptin and insulin assay kits (Linco Research Immunoassay, St. Charles, MO). Serum low-density lipoprotein cholesterol was measured by the direct enzymatic method[14] with Cholestest LDL (Daiichi Pure Chemicals Co., Ltd, Tokyo, Japan). Serum very low–density lipoprotein (VLDL) cholesterol was separated by a modification of the method of Hatch and Lees.[15] A commercially available enzyme-linked immunosorbent assay kit was used to determine serum tumor necrosis factor-α (TNF-α).

Table 1. Primer and Taqman Probe Sequences for Real-Time PCR

Gene	Sense primer (5′-3′)	Antisense primer (5′-3′)	Taqman probe (5′-3′)
c-Met	5′-CGACATTCAGTCCGAGGTTCA-3′	5′-GGGACACTGGCCTGACTCTTC-3′	5′-TGCATGTTCTCCCCACTTGCGG-3′
HGF	5′-GACATGTCTTGCCTGATTCTGTGT-3′	5′-AGTCTGTGACATTCCTCAGTGTTCA-3′	5′-TCACCGTTGCAGGTCATGCATTCA-3′
HOX1	5′-CACCTTCCCGAGCATCGA-3′	5′-AGGCGGTCTTAGCCTCTTCTGT-3′	5′-CTCGCATGAACACTCTGGAGATGACC-3′
MT1	5′-CTGCTCCACCGGCGG-3′	5′-GCCCTGGGCACATTTGG-3′	5′-CTCCTGCAAGAAGAGCTGCTGCTCCT-3′
MT2	5′-TCCTGTGCCACAGATGGATC-3′	5′-GTCCGAAGCCTCTTTGCAGA-3′	5′-AAAGCTGCTGTTCCTGCTGCCCC-3′
SREBP1a	5′-ACACAGCGGTTTTGAACGACA-3′	5′-GCATCAAATAGGCCAGGGAA-3′	5′-CATGCTTCAGCTCATCAACAACCAAG-3′
SREBP1c	5′-GGAGCCATGGATTGCACATT-3′	5′-GCATCAAATAGGCCAGGGAA-3′	5′-CATGCTTCAGCTCATCAACAACCAAG-3′
SCD1	5′-CCTCATCATTGCCAACACCAT-3′	5′-AGCCAACCCACGTGAGAGAA-3′	5′-TTCTCTGAGACACACGCCGACCCTC-3′
SCD2	5′-ACCGCTGGCACATCAACTTC-3′	5′-GGACACCCTCTTCCGGTCAT-3′	5′-CCACGTTCTTCATCGACTGCATGGC-3′

Real-Time Quantitative PCR Analysis

Total RNA was extracted from the liver with ISOGEN (Nippon Gene, Tokyo, Japan) according to the method of Chomczynski and Sacchi, as previously described.[16] For the reverse-transcriptase reaction, TaqMan reverse transcription reagents (Applied Biosystems, Foster City, CA) were used. Briefly, the reverse-transcriptase reaction (final volume of 50 μL) was conducted for 60 minutes at 37°C followed by 25°C for 10 minutes using random hexamers. Polymerase chain reaction (PCR) amplification was performed with TaqMan Universal Master Mix (Applied Biosystems). In brief, reactions were performed in duplicate containing 2× Universal PCR master mix, 2 μL of template cDNA, 900 nmol/L of primers, and 250 nmol/L of probe in a final volume of 50 μL and were analyzed in a 96-well optical reaction plate (Applied Biosystems). Primers and probes were synthesized by Applied Biosystems custom oligo synthesis service. Sequences of primers and probes are shown in Table 1. Probes include a fluorescent reporter dye, FAM, on the 5′ end and labeled with fluorescent quencher dye, TAMRA, on the 3′ end to allow direct detection of the PCR product. Reactions were amplified and quantified using an ABI 7700 sequence detector and manufacturer's software (Applied Biosystems). The threshold cycle (Ct) indicates the fractional cycle number at which the amount of amplified target reaches a fixed threshold. The relative quantity of target messenger RNA (mRNA) was obtained using the comparative Ct method and was normalized using predeveloped TaqMan assay reagent rat 18S ribosomal RNA as an endogenous control (Applied Biosystems) (for details, see user Bulletin 2 for the ABI PRISM 7700 Sequence Detection System under www.appliedbiosystems.com/support/tutorials). Briefly, the TaqMan software (Applied Biosystem) was used to calculate a Ct value for each reaction, where the Ct value is the point in the extension phase of the PCR reaction that the product is distinguishable from the background. The Ct values were then normalized for amplification by subtracting the Ct value calculated for 18S ribosomal RNA, an endogenous control for the amount of mRNA from the same sample, to obtain a Ct using the following equation: Ct target − Ct 18S ribosomal RNA = Ct. The fold induction was calculated relative to the Ct value obtained in the control rats or cells. The normalized expression was calculated as fold changes in a quantity of mRNA. TNF-α mRNA was measured using predeveloped TaqMan assay reagent rat TNF-α (Applied Biosystems) (for details, see user Bulletin 2 for the ABI PRISM 7700 Sequence Detection System under www.appliedbiosystems.com/support/tutorials).

Isolation and Primary Culture of Rat Hepatocytes

Primary cultured hepatocytes were prepared from livers of ethanol-fed rats through a collagenase perfusion method in group A as described elsewhere.[17] The isolated hepatocytes were cultured on gelled pig tendon collagen (Cellmatrix, Nitta zerachin, Ltd., Osaka, Japan), and the second layer of collagen gel was spread over the cells after 1 day of incubation as previously described.[17] A PPARγ-selective agonist AD4833 (pioglitazone hydrochloride, Takeda, Ltd., Osaka, Japan)[18] and troglitazone (Sankyo, Ltd., Tokyo, Japan)[5] was dissolved in dimethyl sulfoxide (DMSO) and added to the hepatocytes at various doses in a volume at 0.05% of the medium. In the control, the medium was supplemented with the same volume of DMSO.

Transcriptome Analyses by DNA Microarray

Transcriptome analyses were performed by using DNA microarrays (Atlas cDNA expression arrays, Clontech). Preparation of ^{33}P-labeled cDNA samples, hybridization, and washing were carried out with total RNA of the liver tissue according to the manufacturer's manual. All data sets were normalized to the signal density of housekeeping genes, such as the gene encoding glyceraldehyde-3-phosphate dehydrogenase, and total radioactivity, which represents the total amount of cDNA hybridized to the microarrays. The threshold for determining the significance of changes in the level of gene expression was established by using an algorithm that requires both a significant absolute and significant fold change.[19,20]

Western and Immunoprecipitation Analysis

Total cellular protein (50 μg) collected from snap-frozen liver was subjected to Western blot analysis for c-Met, mature hepatocyte growth factor (HGF), and apolipoprotein B (apoB)100. For immunoblot analyses, primary antisera were used at the concentration of 1:100. The membranes were

probed with antirat c-Met antibody (Santa Cruz Biotechnology, Santa Cruz, CA), anti-rat HGFα antibody (Santa Cruz Biotech), and anti-rat apoB antibody (Santa Cruz Biotech). For immunoprecipitation, lysates (10 mg of protein) were incubated with protein A-agarose beads (Pierce, Rockford, IL) to precipitate the antigen-antibody complex. Samples were separated by SDS-PAGE on 10% polyacryamide gels. After electrophoresis, the gel was transferred to polyvinylidine difluoride sheets, which were subsequently probed with anti-phosphotyrosine antibody (PY-20; ICN Biomedicals Inc., Aurora, OH) or antirat c-Met antibody. Then, they were incubated with a chemiluminescence substrate (ECL reagent: Amersham Life Science, Buckinghamshire, UK) and exposed to Hyperfilm-MP (Amersham). Densitometric analysis was performed with National Institutes of Health Image Data analysis software.

Immunohistochemistry

For detection of 4-hydroxynonenal (4-HNE) protein adducts, paraffinized sections were deparaffinized, rehydrated, treated with normal horse serum, and incubated with mAb anti-4-HNE (0.625 μg/mL) (Nippon Rouka Seigyo Kenkyuujo, Tokyo, Japan) overnight at 4°C. After several washes with phophate-buffered saline, the sections were stained with biotinylated antimouse IgG for 1 hour (Vectastain Elite ABC kit; Vector Laboratories, Inc., Burlingame, CA). To prevent endogenous peroxidase reactions, the samples were pretreated with 0.3% H_2O_2 in cold methanol for 30 minutes and were subsequently incubated with avidin and horseradish peroxidase (HRP)-conjugated biotin for 30 minutes, followed by detection with 3,3′-diaminobenzidine solution containing 0.003% H_2O_2.

Measurement of DNA Synthesis

DNA synthesis was measured by bromodeoxyuridine (BrdU) incorporation with a Cell Proliferation ELISA, BrdU kit (Roche Molecular Biochemicals, Mannheim, Germany). In brief, hepatocytes were suspended in William's medium E supplemented with 10% fetal bovine serum (FBS), 10 nmol/L insulin, 10 nmol/L dexamethasone, penicillin (5 U/mL), and streptomycin (50 μg/mL) and seeded at a density of 5×10^4 cells/cm^2 on collagen-coated dishes. The culture medium was exchanged after 4 hours for William's medium E supplemented with 10% FBS. After incubation in William's medium E with 10% FBS for approximately 20 hours, the culture medium was exchanged for William's medium E containing 10% FBS with HGF/SF, pioglitazone, or both. They were then cultured for another 24 hours with the addition of BrdU and were harvested in determining the BrdU incorporation into cellular DNA according to the manufacturer's instructions.

Analyses for Effects of Pioglitazone on Ethanol Metabolism in Rats

Four-week-old male Sprague–Dawley rats were randomly divided into 2 groups: rats fed the Lieber–DeCarli control liquid diet for 10 days (n = 16) and those pair fed isocaloric control liquid diet for 10 days during which they were given pioglitazone (10 mg/kg body weight/day) once every 24 hours intragastrically (n = 16). After overnight starvation, rats were given ethanol intragastrically at 4 g/kg body weight on the 10th day. Before and 2, 12, and 24 hours after the ethanol administration, 4 rats in each group were sacrificed to collect heparinized blood samples which were immediately deproteinized to determine ethanol and acetaldehyde concentrations through gas chromatography.[21]

Statistical Analysis

All data are expressed as the mean ± standard error. Statistical analysis was performed by using the unpaired Student t test or by 1-way analysis of variance. When the analysis of variance analyses were applied, differences in mean values among groups were examined by Fisher's multiple comparison test.

Results

Pioglitazone Attenuates Hepatic Steatosis Caused by Chronic Ethanol Administration

The hepatic triglyceride concentration in rats given the isocaloric pair fed liquid diet was 9.67 (±4.34) mg/g liver weight, as opposed to 78.24 (±11.25) mg/g liver weight in the rats given the ethanol-containing diet for 6 weeks (Table 2). Histological analysis showed that lipid droplets accumulated in the hepatocytes in pericentral regions but not in those in periportal regions in the ethanol-fed rats. On the other hand, such changes were not notable in the control liver even with the lipid-specific oil red staining (Figure 1). Pioglitazone (10 mg/kg per day) markedly decreased accumulation of lipid droplets in both perivenular and the periportal regions with the total body weight remaining unchanged (Figure 1). In good agreement with these results, hepatic triglyceride levels became as low as in the pair-fed control rats (Table 2). Treatment with methylcellulose as a vehicle had no effect on either triglyceride contents or histology in the liver (data not shown). The ethanol feeding caused an increase in the liver weight/body weight ratio and a decrease in the epididymal fat weight/body weight ratio, whereas pioglitazone treatment prevented these changes (Table 2).

Analyses of serum AST and ALT activity to assess the effect of pioglitazone on liver function showed that pioglitazone suppressed the elevation of serum concentrations of AST and ALT in ethanol-fed rats (Table 2), and this improvement was associated with improvement in histological findings in the liver. Ethanol feeding caused elevations of the serum concentrations of free fatty acids,